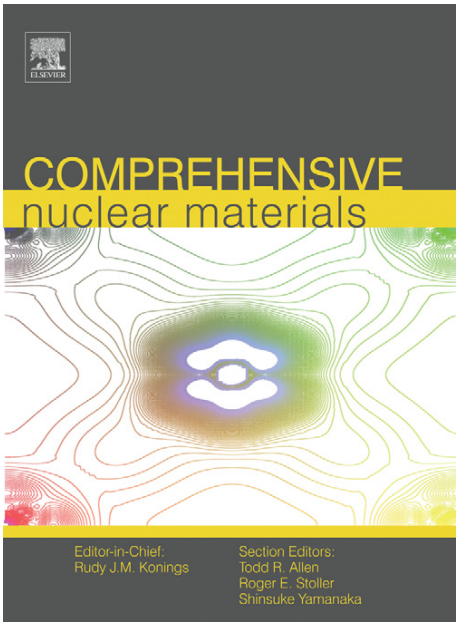

Golubov S.I., Barashev A.V., and Stoller R.E. (2012) Radiation Damage Theory. In: Konings R.J.M., (ed.) Comprehensive Nuclear Materials, volume 1, pp. 357-391 Amsterdam: Elsevier.

1.13 Radiation Damage Theory

S. I. Golubov
Oak Ridge National Laboratory, Oak Ridge, TN, USA
A. V. Barashev
Oak Ridge National Laboratory, Oak Ridge, TN, USA; University of Tennessee, Knoxville, TN, USA
R. E. Stoller
Oak Ridge National Laboratory, Oak Ridge, TN, USA

Published by Elsevier Ltd.

Comprehensive Nuclear Materials (2012), vol. 1, pp. 357-391

Abbreviations

bcc	Body-centered cubic
BEK	Bullough, Eyre, and Krishan (model)
fcc	Face-centered cubic
F–P	Fokker–Plank equation
FP	Frenkel pair
FP3DM	Frenkel pair three-dimensional diffusion model
GB	Grain boundary
hcp	Hexagonal close-packed
kMC	Kinetic Monte Carlo
MD	Molecular dynamics
ME	Master equation
MFA	Mean-field approximation
NRT	Norgett, Robinson, and Torrens (standard)
PBM	Production bias model
PD	Point defect
PKA	Primary knock-on atom
RDT	Radiation damage theory
RIS	Radiation-induced segregation
RT	Rate theory
SDF	Size distribution function
SFT	Stacking-fault tetrahedron
SIA	Self-interstitial atom

Symbols

C_α	Concentration of α-type defects
D_α	Diffusion coefficient for α-type defects
$f(r_i)$	Size distribution function
G_α	Production rate of α-type defects by irradiation
N	Number density
r	Mean void radius
R	Reaction rate
r_d	Dislocation capture radius for an SIA cluster
s	Void swelling level
Λ	Total trap density in one dimension
Λ_j	Partial density of traps of kind j ($j = c, d$)
ρ_d	Dislocation density
τ	Lifetime

1.13.1 Introduction

The study of radiation effects on the structure and properties of materials started more than a century ago,[1] but gained momentum from the development of fission reactors in the 1940s. In 1946, Wigner[2] pointed out the possibility of a deleterious effect on material properties at high neutron fluxes, which was then confirmed experimentally.[3] A decade later, Konobeevsky *et al.*[4] discovered irradiation creep in fissile metallic uranium, which was then observed in stainless steel.[5] The discovery of void swelling in neutron-irradiated stainless steels in 1966 by Cawthorne and Fulton[6] demonstrated that radiation effects severely restrict the lifetime of reactor materials and that they had to be systematically studied.

The 1950s and early 1960s were very productive in studying crystalline defects. It was recognized that atoms in solids migrate via vacancies under thermal-equilibrium conditions and via vacancies and self-interstitial atoms (SIAs) under irradiation; also that the bombardment with energetic particles generates high concentrations of defects compared to equilibrium values, giving rise to radiation-enhanced diffusion. Numerous studies revealed the properties of point defects (PDs) in various crystals. In particular, extensive studies of annealing of irradiated samples resulted in categorizing the so-called 'recovery stages' (e.g., Seeger[7]), which comprised a solid basis for understanding microstructure evolution under irradiation.

Already by this time, which was well before the discovery of void swelling in 1966, the process of interaction of various energetic particles with solid

targets had been understood rather well (e.g., Kinchin and Pease[8] for a review). However, the primary damage produced was wrongly believed to consist of Frenkel pairs (FPs) only. In addition, it was commonly believed that this damage would not have serious long-term consequences in irradiated materials. The reasoning was correct to a certain extent; as they are mobile at temperatures of practical interest, the irradiation-produced vacancies and SIAs should move and recombine, thus restoring the original crystal structure. Experiments largely confirmed this scenario, most defects did recombine, while only about 1% or an even smaller fraction survived and formed vacancy and SIA-type loops and other defects. However small, this fraction had a dramatic impact on the microstructure of materials, as demonstrated by Cawthorne and Fulton.[6] This discovery initiated extensive experimental and theoretical studies of radiation effects in reactor materials which are still in progress today.

After the discovery of swelling in stainless steels, it was found to be a general phenomenon in both pure metals and alloys. It was also found that the damage accumulation takes place under irradiation with any particle, provided that the recoil energy is higher than some displacement threshold value, E_d, (~30–40 eV in metallic crystals). In addition, the microstructure of different materials after irradiation was found to be quite similar, consisting of voids and dislocation loops. Most surprisingly, it was found that the microstructure developed under irradiation with ~1 MeV electrons, which produces FPs only, is similar to that formed under irradiation with fast neutrons or heavy-ions, which produce more complicated primary damage (see Singh *et al.*[1]). All this created an illusion that three-dimensional migrating (3D) PDs are the main mobile defects under any type of irradiation, an assumption that is the foundation of the initial kinetic models based on reaction rate theory (RT). Such models are based on a mean-field approximation (MFA) of reaction kinetics with the production of only 3D migrating FPs. For convenience, we will refer to these models as FP production 3D diffusion model (FP3DM) and henceforth this abbreviation will be used. This model was developed in an attempt to explain the variety of phenomena observed: radiation-induced hardening, creep, swelling, radiation-induced segregation (RIS), and second phase precipitation. A good introduction to this theory can be found, for example, in the paper by Sizmann,[9] while a comprehensive overview was produced by Mansur,[10] when its development was already completed. The theory is rather simple, but its general methodology can be useful in the further development of radiation damage theory (RDT). It is valid for ~1 MeV electron irradiation and is also a good introduction to the modern RDT, see **Section 1.13.5**.

Soon after the discovery of void swelling, a number of important observations were made, for example, the void super-lattice formation[11–14] and the micrometer-scale regions of the enhanced swelling near grain boundaries (GBs).[15] These demonstrated that under neutron or heavy-ion irradiation, the material microstructure evolves differently from that predicted by the FP3DM. First, the spatial arrangement of irradiation defects voids, dislocations, second phase particles, etc. is not random. Second, the existence of the micrometer-scale heterogeneities in the microstructure does not correlate with the length scales accounted for in the FP3DM, which are an order of magnitude smaller. Already, Cawthorne and Fulton[6] in their first publication on the void swelling had reported a nonrandomness of spatial arrangement of voids that were associated with second phase precipitate particles. All this indicated that the mechanisms operating under cascade damage conditions (fast neutron and heavy-ion irradiations) are different from those assumed in the FP3DM. This evidence was ignored until the beginning of the 1990s, when the production bias model (PBM) was put forward by Woo and Singh.[16,17] The initial model has been changed and developed significantly since then[18–28] and explained successfully such phenomena as high swelling rates at low dislocation density (**Section 1.13.6.2.2**), grain boundary and grain-size effects in void swelling, and void lattice formation (**Section 1.13.6.2.3**). An essential advantage of the PBM over the FP3DM is the two features of the cascade damage: (1) the production of PD clusters, in addition to single PDs, directly in displacement cascades, and (2) the 1D diffusion of the SIA clusters, in addition to the 3D diffusion of PDs (**Section 1.13.3**). The PBM is, thus, a generalization of the FP3DM (and the idea of intracascade defect clustering introduced in the model by Bullough *et al.* (BEK[29])). A short overview of the PBM was published about 10 years ago.[1] Here, it will be described somewhat differently, as a result of better understanding of what is crucial and what is not, see **Section 1.13.6**.

From a critical point of view, it should be noted that successful applications of the PBM have been limited to low irradiation doses (<1 dpa) and pure metals (e.g., copper). There are two problems that

prevent it from being used at higher doses. First, the PBM in its present form[1] predicts a saturation of void size (see, e.g., Trinkaus *et al.*[19] and Barashev and Golubov[30] and Section 1.13.6.3.1). This originates from the mixture of 1D and 3D diffusion–reaction kinetics under cascade damage conditions, hence from the assumption lying at the heart of the model. In contrast, experiments demonstrate unlimited void growth at high doses in the majority of materials and conditions (see, e.g., Singh *et al.*,[31] Garner,[32] Garner *et al.*,[33] and Matsui *et al.*[34]). An attempt to resolve this contradiction was undertaken[23,25,27] by including thermally activated rotations of the SIA-cluster Burgers vector; but it has been shown[25] that this does not solve the problem. Thus, the PBM in its present form fails to account for the important and common observation: the indefinite void growth under cascade irradiation. The second problem of the PBM is that it fails to explain the swelling saturation observed in void lattices (see, e.g., Kulchinski *et al.*[13]). In contrast, it predicts even higher swelling rates in void lattices than in random void arrangements.[25] This is because of free channels between voids along close-packed directions, which are formed during void ordering and provide escape routes for 1D migrating SIA clusters to dislocations and GBs, thus allowing 3D migrating vacancies to be stored in voids.

Resolving these two problems would make PBM self-consistent and complete its development. A solution to the first problem has recently been proposed by Barashev and Golubov[35,36] (see Section 1.13.7). It has been suggested that one of the basic assumptions of all current models, including the PBM, that a random arrangement of immobile defects exists in the material, is correct at low and incorrect at high doses. The analysis includes discussion of the role of RIS and provides a solution to the problem, making the PBM capable of describing swelling in both pure metals and alloys at high irradiation doses. The solution for the second problem of the PBM mentioned above is the main focus of a forthcoming publication by Golubov *et al.*[37]

Because of limitations of space, we only give a short guide to the main concepts of both old and more recent models and the framework within which radiation effects, such as void swelling, and hardening and creep, can be rationalized. For the same reason, the impact of radiation on reactor fuel materials is not considered here, despite a large body of relevant experimental data and theoretical results collected in this area.

1.13.2 The Rate Theory and Mean Field Approximation

The RDT is frequently but inappropriately called 'the rate theory.' This is due to the misunderstanding of the role of the transition state theory (TST) or (chemical reaction) RT (see Laidler and King[38] and Hänggi *et al.*[39] for reviews) in the RDT. The TST is a seminal scientific contribution of the twentieth century. It provides recipes for calculating reaction rates between individual species of the types which are ubiquitous in chemistry and physics. It made major contributions to the fields of chemical kinetics, diffusion in solids, homogeneous nucleation, and electrical transport, to name a few. TST provides a simple way of formulating reaction rates and gives a unique insight into how processes occur. It has survived considerable criticisms and after almost 75 years has not been replaced by any general treatment comparable in simplicity and accuracy. The RDT uses TST as a tool for describing reactions involving radiation-produced defects, but cannot be reduced to it. This is true for both the mean-field models discussed here, and the kinetic Monte Carlo (kMC) models that are also used to simulate radiation effects (see **Chapter 1.14, Kinetic Monte Carlo Simulations of Irradiation Effects**).

The use of the name RT also created an incorrect identification of the RDT with the models that emerged in the very beginning, which assumed the production of only FPs and 3D migrating PDs to be the only mobile species, that is, FP3DM. It failed to appreciate the importance of numerous contradicting experimental data and, hence, to produce significant contribution to the understanding of neutron irradiation phenomena (see Barashev and Golubov[35] and Section 1.13.6). A common perception that the RDT in general is identical to the FP3DM has developed over the years. So, the powerful method was rejected because of the name of the futile model. This caused serious damage to the development of RDT during the last 15 years or so. Many research proposals that included it as an essential part, were rejected, while simulations, for example, by the kMC etc. were aimed at substituting the RDT. The simulations can, of course, be useful in obtaining information on processes on relatively small time and length scales but cannot replace the RDT in the large-scale predictions. The RDT and any of its future developments will necessarily use TST.

An important approximation used in the theory is the MFA. The idea is to replace all interactions in a

many-body system with an effective one, thereby reducing the problem of one-body in an effective field. The MFA is used in different areas of physics on all scales: from *ab initio* to continuum models. In the RDT, the main objective is to describe diffusion and interaction between defects in a self-consistent way. So, the primary damage is produced by irradiation in the form of mobile vacancies, SIAs, SIA clusters, and immobile defects. The latter together with preexisting dislocations and GBs, and those formed during irradiation, for example, voids and dislocation loops of different sizes represent crystal microstructure and change during irradiation. The complete problem of microstructure evolution is, thus, too complex; some approximations are necessary and the MFA is the most natural option.

It should be emphasized that a particular realization of the MFA depends on the problem and it can be employed even in cases with spatial correlations between defects. For example, in this way Gösele[40] demonstrated that the absorption rates of 3D migrating vacancies by randomly distributed and ordered voids are significantly different; and then it was shown in Barashev *et al.*[25] that the effect is even stronger for 1D diffusing SIA clusters. In some specific cases, however, when the time and length scales of the problem permit, numerical approaches such as kMC can be a natural choice for studying spatial correlations.

1.13.3 Defect Production

Interaction of energetic particles with a solid target is a complex process. A detailed description is beyond the scope of the present paper (Robinson[41]). However, the primary damage produced in collision events is the main input to the RDT and is briefly introduced here. Energetic particles create primary knock-on (or recoil) atoms (PKAs) by scattering either incident radiation (electrons, neutrons, protons) or accelerated ions. Part of the kinetic energy, E_{PKA}, transmitted to the PKA is lost to the electron excitation. The remaining energy, called the damage energy, T_{d}, is dissipated in elastic collisions between atoms. If the T_{d} exceeds a threshold displacement energy, E_{d}, for the target material, vacancy-interstitial (or Frenkel) pairs are produced. The total number of displaced atoms is proportional to the damage energy in a model proposed by Norgett *et al.*[42] and known as the NRT standard

$$\nu(\tilde{E}) = 0.8\frac{E^{\mathrm{PKA}}(\tilde{E})}{2E_{\mathrm{d}}} \qquad [1]$$

The total production rate of displacements per atom (dpa), G^{NRT}, can be calculated using this equation, by integrating the flux of projectile particles, $\varphi(E)$, (E is the particle energy), as

$$G^{\mathrm{NRT}} = \int_0^{\infty} \mathrm{d}E\varphi(E) \int_{E_{\mathrm{d}}}^{\tilde{E}^{\max}} \frac{\mathrm{d}\sigma(E,\tilde{E})}{\mathrm{d}\tilde{E}}\nu(\tilde{E})\mathrm{d}\tilde{E} \qquad [2]$$

where $\sigma(E,\tilde{E})$ is the cross-section of reactions, in which an incident particle transfers energy $\tilde{E}$ to an atom and $\tilde{E}^{\max}$ is the maximum transferable energy. For a head-on collision of a nonrelativistic projectile of mass m and a target atom of mass M

$$\tilde{E}^{\max} = \frac{4Mm}{(M+m)^2}E \qquad [3a]$$

while for relativistic electrons,

$$\tilde{E}^{\max} = \frac{2m_{\mathrm{e}}}{M}\left(\frac{E}{m_{\mathrm{e}}c^2}+2\right)E \qquad [3b]$$

where m_{e} is the electron mass and c is the speed of light.

The NRT model is accepted as an international standard for quantifying the number of atomic displacements produced under cascade damage conditions. It is based on the theory of isolated binary collisions and, hence, cannot be used to characterize the defects formed during the collision phase and survive at the end of the cool-down phase of cascades. Description of the latter is considered below.

1.13.3.1 Characterization of Cascade-Produced Primary Damage

The NRT displacement model is most correct for irradiation such as 1 MeV electrons, which produce only low-energy recoils and, therefore, the FPs. At higher recoil energies, the damage is generated in the form of displacement cascades, which change both the production rate and the nature of the defects produced. Over the last two decades, the cascade process has been investigated extensively by molecular dynamics (MD) and the relevant phenomenology is described in **Chapter 1.11, Primary Radiation Damage Formation** and recent publications.[43,44] For the purpose of this chapter the most important findings are (see discussion in the **Chapter 1.11, Primary Radiation Damage Formation**):

- For energy above ~0.5 keV, the displacements are produced in cascades, which consist of a collision and recovery or cooling-down stage.

- A large fraction of defects generated during the collision stage of a cascade recombine during the cooling-down stage. The surviving fraction of defects decreases with increasing PKA energy up to ~10 keV, when it saturates at a value of ~30% of the NRT value, which is similar in several metals and depends only slightly on the temperature.
- By the end of the cooling-down stage, both SIA and vacancy clusters can be formed. The fraction of defects in clusters increases when the PKA energy is increased and is somewhat higher in face-centered cubic (fcc) copper than in bcc iron.
- The SIA clusters produced may be either glissile or sessile. The glissile clusters of large enough size (e.g., >4 SIAs in iron) migrate 1D along close-packed crystallographic directions with a very low activation energy, practically a thermally, similar to the single crowdion.[45,46] The SIA clusters produced in iron are mostly glissile, while in copper they are both sessile and glissile.
- The vacancy clusters produced may be either mobile or immobile vacancy loops, stacking-fault tetrahedra (SFTs) in fcc metals, or loosely correlated 3D arrays in bcc materials such as iron.

As compared to the FP production, the cascade damage has the following features.

- The generation rates of single vacancies and SIAs are not equal: $G_v \neq G_i$ and both smaller than that given by the NRT standard, eqn. [2]: $G_v, G_i < G^{NRT}$.
- Mobile species consist of 3D migrating single vacancies and SIAs, and 1D migrating SIA and vacancy clusters.
- Sessile vacancy and SIA clusters, which can be sources/sinks for mobile defects, can be formed.

The rates of PD production in cascades are given by

$$G_v = G^{NRT}(1-\varepsilon_r)(1-\varepsilon_v) \quad [4]$$

$$G_i = G^{NRT}(1-\varepsilon_r)(1-\varepsilon_i) \quad [5]$$

where ε_r is the fraction of defects recombined in cascades relative to the NRT standard value, and ε_v and ε_i are the fractions of clustered vacancies and SIAs, respectively.

One also needs to introduce parameters describing mobile and immobile vacancy and SIA-type clusters of different size. The production rate of the clusters containing x defects, $G(x)$, depends on cluster type, PKA energy and material, and is connected with the fractions ε as

$$\sum_{x=2}^{\infty} xG_\alpha(x) = \varepsilon_\alpha G^{NRT}(1-\varepsilon_r) \quad [6]$$

where $\alpha = v, i$ for the vacancy and SIA-type clusters, respectively. The total fractions ε_v and ε_i of defects in clusters are given by the sums of those for mobile and immobile clusters,

$$\varepsilon_\alpha = \varepsilon_\alpha^s + \varepsilon_\alpha^g \quad [7]$$

where the superscripts 's' and 'g' indicate sessile and glissile clusters, respectively. In the mean-size approximation

$$G_\alpha^j(x) = G_\alpha^j \delta\left(x - \langle x_\alpha^j \rangle\right) \quad [8]$$

where $j = s, g$; $\delta(x)$ is the Kronecker delta and $\langle x_\alpha^j \rangle$ is the mean cluster size and

$$G_\alpha^j = \langle x_\alpha^j \rangle^{-1} G^{NRT}(1-\varepsilon_r)\varepsilon_\alpha^j \quad [9]$$

Also note that although MD simulations[46] show that small vacancy loops can be mobile, this has not been incorporated into the theory yet and we assume that they are sessile: $\varepsilon_v^g = 0$ and $\varepsilon_v^s = \varepsilon_v$.

1.13.3.2 Defect Properties

Single vacancies and other vacancy-type defects, such as, SFTs and dislocation loops, have been considered quite extensively since the 1930s because it was recognized that they define many properties of solids under equilibrium conditions. Extensive information on defect properties was collected before material behavior in irradiation environments became a problem of practical importance. Qualitatively new crystal defects, SIAs and SIA clusters, were required to describe the phenomena in solids under irradiation conditions. This has been studied comprehensively during the last ~40 years. The properties of these defects and their interaction with other defects are quite different compared to those of the vacancy-type. Correspondingly, the crystal behavior under irradiation is also qualitatively different from that under equilibrium conditions. The basic properties of vacancy- and SIA-type defects are summarized below.

1.13.3.2.1 Point defects

The basic properties of PDs are as follows:

1. Both vacancies and SIAs are highly mobile at temperatures of practical interest, and the diffusion coefficient of SIAs, D_i, is much higher than that of vacancies, D_v : $D_i \gg D_v$.

2. The relaxation volume of an SIA is much larger than that of a vacancy, resulting in higher interaction energy with edge dislocations and other defects.
3. Vacancies and SIAs are defects of opposite type, and their interaction leads to mutual recombination.
4. SIAs, in contrast to vacancies, may exist in several different configurations providing different mechanisms of their migration.
5. PDs of both types are eliminated at fixed sinks, such as voids and dislocations.

The first property leads to a specific temperature dependence of the damage accumulation: only limited number of defects can be accumulated at irradiation temperature below the recovery stage III, when vacancies are immobile. At higher temperature, when both PDs are mobile, the defect accumulation is practically unlimited. The second property is the origin of the so-called 'dislocation bias' (see **Section 1.13.5.2**) and, as proposed by Greenwood *et al.*,[47] is the reason for void swelling. A similar mechanism, but induced by external stress, was proposed in the so-called 'SIPA' (stress-induced preferential absorption) model of irradiation creep.[48–53] The third property provides a decrease of the number of defects accumulated in a crystal under irradiation. The last property, which is quite different compared to that of vacancies leads to a variety of specific phenomena and will be considered in the following sections.

1.13.3.2.2 Clusters of point defects

The configuration, thermal stability and mobility of vacancy, and SIA clusters are of importance for the kinetics of damage accumulation and are different in the fcc and bcc metals. In the fcc metals, vacancy clusters are in the form of either dislocation loops or SFTs, depending on the stacking-fault energy, and the fraction of clustered vacancies, ε_v, is close to that for the SIAs, ε_i. In the bcc metals, nascent vacancy clusters usually form loosely correlated 3D configurations, and ε_v is much smaller than ε_i. Generally, vacancy clusters are considered to be immobile and thermally unstable above the temperature corresponding to the recovery stage V.

In contrast to vacancy clusters, the SIA clusters are mainly in the form of a 2D bundle of crowdions or small dislocation loops. They are thermally stable and highly mobile, migrating 1D in the close-packed crystallographic directions.[45] The ability of SIA clusters to move 1D before being trapped or absorbed by a dislocation, void, etc. leads to entirely different reaction kinetics as compared with that for 3D migrating defects, and hence may result in a qualitatively different damage accumulation than that in the framework of the FP3DM (see **Section 1.13.6**).

It should be noted that MD simulations provide maximum evidence for the high mobility of small SIA clusters. Numerous experimental data, which also support this statement, are discussed in this chapter, however, indirectly. One such fact is that most of the loops formed during ion irradiations of a thin metallic foil have Burgers vectors lying in the plane of the foil.[54] It should also be noted that recent *in situ* experiments[55–58] provide interesting information on the behavior of interstitial loops (>1 nm diameter, that is, large enough to be observable by transmission electron microscope, TEM). The loops exhibit relatively low mobility, which is strongly influenced by the purity of materials. This is not in contradiction with the simulation data. The observed loops have a large cross-section for interaction with impurity atoms, other crystal imperfections and other loops: all such interactions would slow down or even immobilize interstitial loops. Small SIA clusters produced in cascades consist typically of approximately ten SIAs and have, thus, much smaller cross-sections and consequently a longer mean-free path (MFP). The influence of impurities may, however, be strong on both the mobility of SIA clusters and, consequently, void swelling is yet to be included in the theory.

1.13.4 Basic Equations for Damage Accumulation

Crystal microstructure under irradiation consists of two qualitatively different defect types: mobile (single vacancies, SIAs, and SIA and vacancy clusters) and immobile (voids, SIA loops, dislocations, etc.). The concentration of mobile defects is very small ($\sim 10^{-10}$–10^{-6} per atom), whereas immobile defects may accumulate an unlimited number of PDs, gas atoms, etc. The mathematical description of these defects is, therefore, different. Equations for mobile defects describe their reactions with immobile defects and are often called the rate (or balance) equations. The description of immobile defects is more complicated because it must account for nucleation, growth, and coarsening processes.

1.13.4.1 Concept of Sink Strength

The mobile defects produced by irradiation are absorbed by immobile defects, such as voids, dislocations, dislocation loops, and GBs. Using a MFA, a crystal

can be treated as an absorbing medium. The absorption rate of this medium depends on the type of mobile defect, its concentration and type, and the size and spatial distribution of immobile defects. A parameter called 'sink strength' is introduced to describe the reaction cross-section and commonly designated as k_v^2, k_i^2, and $k_{icl}^2(x)$ for vacancies, SIAs, and SIA clusters of size x (the number of SIAs in a cluster), respectively. The role of the power '2' in these values is to avoid the use of square root for the MFPs of diffusing defects between production until absorption, which are correspondingly k_v^{-1}, k_i^{-1}, and $k_{icl}^{-1}(x)$. There are a number of publications devoted to the derivation of sink strengths.[40,59–61] Here we give a simple but sufficient introduction to this subject.

1.13.4.2 Equations for Mobile Defects

For simplicity, we use the following assumptions:

- The PDs, single vacancies, and SIAs, migrate 3D.
- SIA clusters are glissile and migrate 1D.
- All vacancy clusters, including divacancies, are immobile.
- The reactions between mobile PDs and clusters are negligible.
- Immobile defects are distributed randomly over the volume.

Then, the balance equations for concentrations of mobile vacancies, C_v, SIAs, C_i, and SIA clusters, $C_{icl}^g(x)$, are as follows

$$\frac{dC_v}{dt} = G^{NRT}(1-\varepsilon_r)(1-\varepsilon_v) + G_v^{th} - k_v^2 D_v C_v - \mu_R D_i C_i C_v \quad [10]$$

$$\frac{dC_i}{dt} = G^{NRT}(1-\varepsilon_r)(1-\varepsilon_i) - k_i^2 D_i C_i - \mu_R D_i C_i C_v \quad [11]$$

$$\frac{dC_{icl}^g(x)}{dt} = G_{icl}^g(x) - k_{icl}^2(x) D_{icl} C_{icl}^g, \quad x = 2, 3, \ldots x_{max} \quad [12]$$

where G_v^{th} is the rate of thermal emission of vacancies from all immobile defects (dislocations, GBs, voids, etc.); D_v, D_i, and $D_{icl}(x)$ are the diffusion coefficients of vacancies, single SIAs, and SIA clusters, respectively; and μ_R is the recombination coefficient of PDs. Since the dependence of the cluster diffusivity, $D_{icl}(x)$, and sink strengths, $k_{icl}^2(x)$, on size x is rather weak,[45,46] the mean-size approximation for the SIA clusters may be used, where all clusters are assumed to be of the size $\langle x_i^g \rangle$. In this case, the set of eqn [12] is reduced to the following single equation

$$\frac{dC_{icl}^g}{dt} = \langle x_i^g \rangle^{-1} G^{NRT}(1-\varepsilon_r)\varepsilon_i^g - k_{icl}^2 D_{icl} C_{icl}^g \quad [13]$$

where eqn [9] is used for the cluster generation rate. To solve eqns [10]–[13], one needs the sink strengths k_v^2, k_i^2, and k_{icl}^2, the rates of vacancy emission from various immobile defects to calculate G_v^{th}, and the recombination constant, μ_R. The reaction kinetics of 3D diffusing PDs is presented in **Section 1.13.5**, while that of 1D diffusing SIA clusters in **Section 1.13.6**. In the following section, we consider equations governing the evolution of immobile defects, which together with the equations above describe damage accumulation in solids both under irradiation and during aging.

1.13.4.3 Equations for Immobile Defects

The immobile defects are those that preexist such as dislocations and GBs and those formed during irradiation: voids, vacancy- and SIA-type dislocation loops, SFTs, and second phase precipitates. Usually, the defects formed under irradiation nucleate, grow, and coarsen, so that their size changes during irradiation. Hence, the description of their evolution with time, t, should include equations for the size distribution function (SDF), $f(\xi, t)$, where ξ is the cluster size.

1.13.4.3.1 Size distribution function

The measured SDF is usually represented as a function of defect size, for example, radius, $\xi \equiv R : f(R, t)$. In calculations, it is more convenient to use x-space, $\xi \equiv x$, where x is the number of defects in a cluster: $f(x, t)$. The radius of a defect, R, is connected with the number of PDs, x, it contains as:

$$\frac{4\pi}{3}R^3 = x\Omega$$
$$\pi R^2 b = x\Omega \quad [14]$$

for voids and loops, respectively, where Ω is the atomic volume and b is the loop Burgers vector. Correspondingly, the SDFs in R- and x-spaces are related to each other via a simple relationship. Indeed, if small dx and dR correspond to the same cluster group, the number density of this cluster group defined by two functions $f(x)dx$ and $f(R)dR$ must be equal, $f(x)dx = f(R)dR$, which is just a differential form

of the equality of corresponding integrals for the total number density:

$$N = \sum_{x=2}^{\infty} f(x) \approx \int_{x=2}^{\infty} f(x)\mathrm{d}x = \int_{R=R_{\min}}^{\infty} f(R)\mathrm{d}R \quad [15]$$

The relationship between the two functions is, thus,

$$f(R) = f(x)\frac{\mathrm{d}x}{\mathrm{d}R} \quad [16]$$

For voids and dislocation loops

$$f_{\mathrm{c}}(R) = \left(\frac{36\pi}{\Omega}\right)^{1/3} x^{2/3} f_{\mathrm{c}}(x)\Big|_{x=\frac{4\pi R^3}{3\Omega}}$$
$$f_{\mathrm{L}}(R) = \left(\frac{4\pi b}{\Omega}\right)^{1/2} x^{1/2} f_{\mathrm{L}}(x)\Big|_{x=\frac{\pi b R^2}{\Omega}} \quad [17]$$

Note the difference in dimensionality: the units of $f(x)$ are atom^{-1} (or m^{-3}), while $f(R)$ is in m^{-1} atom^{-1} (or m^{-4}), as can be seen from eqn [15]. Also note that these two functions have quite different shapes, see **Figure 1**, where the SDF of voids obtained by Stoller *et al.*[62] by numerical integration of the master equation (ME) (see **Sections 1.13.4.3.2** and **1.13.4.4.3**) is plotted in both R- and x-spaces.

1.13.4.3.2 Master equation

The kinetic equation for the SDF (or the ME) in the case considered, when the cluster evolution is driven by the absorption of PDs, has the following form

$$\frac{\partial f^{\mathrm{s}}(x,t)}{\partial t} = G^{\mathrm{s}}(x) + \mathcal{J}(x-1,t) - \mathcal{J}(x,t), x \geq 2 \quad [18]$$

where $G^{\mathrm{s}}(x)$ is the rate of generation of the clusters by an external source, for example, by displacement cascades, and $\mathcal{J}(x,t)$ is the flux of the clusters in the size-space (indexes 'i' and 'v' in eqn [18] are omitted). The flux $\mathcal{J}(x,t)$ is given by

$$\mathcal{J}(x,t) = P(x,t)f(x,t) - \underline{Q}(x+1,t)f(x+1,t) \quad [19]$$

where $P(x,t)$ and $\underline{Q}(x,t)$ are the rates of absorption and emission of PDs, respectively. The boundary conditions for eqn [18] are as follows

$$f(1) = C$$
$$f(x \to \infty) = 0 \quad [20]$$

where C is the concentration of mobile PDs.

If any of the PD clusters are mobile, additional terms have to be added to the right-hand side of eqn [19] to account for their interaction with immobile defect which will involve an increment growth or shrinkage in the size-space by more that unity (see **Section 1.13.6** and Singh *et al.*[22] for details).

The total rates of PD absorption (superscript $\rightarrow$) and emission ($\leftarrow$) are given by

$$\mathcal{J}_{\mathrm{tot}}^{\rightarrow} = \sum_{x=2}^{\infty} P(x)f(x), \quad \mathcal{J}_{\mathrm{tot}}^{\leftarrow} = \sum_{x=2}^{\infty} \underline{Q}(x)f(x) \quad [21]$$

where the superscript arrows denote direction in the size-space. $\mathcal{J}_{\mathrm{tot}}^{\rightarrow}$ and $\mathcal{J}_{\mathrm{tot}}^{\leftarrow}$ are related to the sink strength of the clusters, thus providing a link between equations for mobile and immobile defects. For example, when voids with the SDF $f_{\mathrm{c}}(x)$ and dislocations are only presented in the crystal and the primary damage is in the form of FPs, the balance equations are

$$\frac{\mathrm{d}C_{\mathrm{v}}}{\mathrm{d}t} = G^{\mathrm{NRT}}(1-\varepsilon_{\mathrm{r}}) - \left[\mu_{\mathrm{R}} D_{\mathrm{i}} C_{\mathrm{i}} C_{\mathrm{v}} + Z_{\mathrm{v}}^{\mathrm{d}} \rho_{\mathrm{d}} D_{\mathrm{v}} (C_{\mathrm{v}} - C_{\mathrm{v0}})\right] - \left[P_{\mathrm{c}}(1) f_{\mathrm{c}}(1,t) - \underline{Q}_{\mathrm{c}}^{\mathrm{v}}(2) f_{\mathrm{c}}(2,t)\right] - \sum_{x=1}^{x=\infty} \left(P_{\mathrm{c}}(x) f_{\mathrm{c}}(x,t) - \underline{Q}_{\mathrm{c}}^{\mathrm{v}}(x+1) f_{\mathrm{c}}(x+1,t)\right) \quad [22]$$

$$\frac{\mathrm{d}C_{\mathrm{i}}}{\mathrm{d}t} = G^{\mathrm{NRT}}(1-\varepsilon_{\mathrm{r}}) - \left[\mu_{\mathrm{R}} D_{\mathrm{i}} C_{\mathrm{i}} C_{\mathrm{v}} + Z_{\mathrm{i}}^{\mathrm{d}} \rho_{\mathrm{d}} D_{\mathrm{i}} C_{\mathrm{i}}\right] - \sum_{x=1}^{x=\infty} \underline{Q}_{\mathrm{c}}^{\mathrm{i}}(x+1) f_{\mathrm{c}}(x+1,t) \quad [23]$$

where ρ_{d} and $Z_{\mathrm{i,v}}^{\mathrm{d}}$ are the dislocation density and its efficiencies for absorbing PDs, μ_{R}, is the recombination constant (see **Section 1.13.5**); the last two terms in eqn [22] describe the absorption and

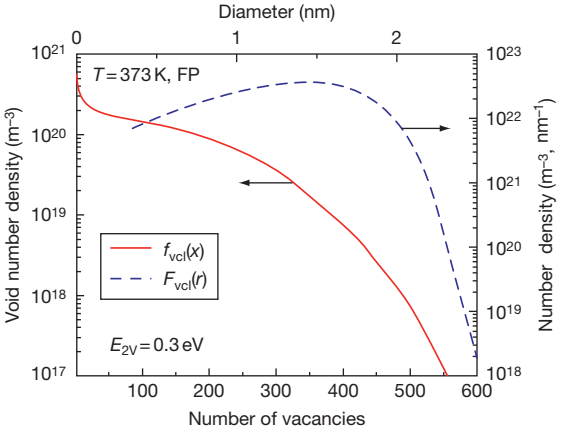

Figure 1 Size distribution function of voids calculated in x-space, $f_{\mathrm{vcl}}(x)$ (x is the number of vacancies), and in d-space, $f_{\mathrm{vcl}}(d)$ (d is the void diameter). From Stoller *et al.*[62]

emission of vacancies by voids and the last term in eqn [23] describes the absorption of SIAs by voids. The balance equations for dislocation loops and secondary phase precipitations can be written in a similar manner. Expressions for the rates $P(x,t), Q(x,t)$, the dislocation capture efficiencies, $Z_{i,v}^{d}$, and μ_R are derived in **Section 1.13.5**.

1.13.4.3.3 Nucleation of point defect clusters

Nucleation of small clusters in supersaturated solutions has been of significant interest to several generations of scientists. The kinetic model for cluster growth and the rate of formation of stable droplets in vapor and second phase precipitation in alloys during aging was studied extensively. The similarity to the condensation process in supersaturated solutions allows the results obtained to be used in RDT to describe the formation of defect clusters under irradiation.

The initial motivation for work in this area was to derive the nucleation rate of liquid drops. Farkas[63] was first to develop a quantitative theory for the so-called homogeneous cluster nucleation. Then, a great number of publications were devoted to the kinetic nucleation theory, of which the works by Becker and Döring,[64] Zeldovich,[65] and Frenkel[66] are most important. Although these publications by no means improved the result of Farkas, their treatment is mathematically more elegant and provided a proper background for subsequent works in formulating ME and revealing properties of the cluster evolution. A quite comprehensive description of the nucleation phenomenon was published by Goodrich.[67,68] Detailed discussions of cluster nucleation can also be found in several comprehensive reviews.[69,70] Generalizations of homogeneous cluster nucleation for the case of irradiation were developed by Katz and Wiedersich[71] and Russell.[72] Here we only give a short introduction to the theory.

For small cluster sizes at high enough temperature, when the thermal stability of clusters is relatively low, the diffusion of clusters in the size-space governs the cluster evolution, which is nucleation of stable clusters. In cases where only FPs are produced by irradiation, the first term on the right-hand side of eqn [18] is equal to zero and cluster nucleation, for example, voids, proceeds via interaction between mobile vacancies to form divacancies, then between vacancies and divacancies to form trivacancies, and so on. By summing eqn [18] from $x = 2$ to ∞, one finds

$$\frac{dN_c}{dt} = \mathcal{J}(x)_{|x=1} \equiv \mathcal{J}_c^{nucl} \qquad [24]$$

where $N_c = \sum_{x=2}^{\infty} f(x)$ is the total number of clusters. The nucleation rate in this case, $\mathcal{J}_c^{nucl}$, is equal to the rate of production of the smallest cluster (divacancies in the case considered); hence the flux $\mathcal{J}(x)_{|x=1}$ is the main concern.

When calculating $\mathcal{J}_c^{nucl}$, one can obtain two limiting SDFs that correspond to two different steady-state solutions of eqn [18]: (1) when the flux $\mathcal{J}(x,t) = 0$, for which the corresponding SDF is $n(x)$, and, (2) when it is a constant: $\mathcal{J}(x,t) = \mathcal{J}_c$, with the SDF denoted as $g(x)$. Let us first find $n(x)$. Using equation $P(x)n(x) - Q(x+1)n(x+1,t) = 0$ and the condition $n(1) = C$, one finds that

$$n(x) = C\prod_{y=1}^{x-1}\frac{P(y)}{Q(y+1)}, x \geq 2 \qquad [25]$$

Using function $n(x)$, the flux $\mathcal{J}(x,t)$ can be derived as follows

$$\mathcal{J}(x,t) = P(x)n(x)\left(\frac{f(x)}{n(x)} - \frac{f(x+1)}{n(x+1)}\right) \qquad [26]$$

The SDF $g(x)$ corresponding to the constant flux, $\mathcal{J}(x,t) = \mathcal{J}_c$, can be found from eqn [26]:

$$g(x) = \mathcal{J}_c n(x)\sum_{y=x}^{\infty}\frac{1}{P(y)n(y)} \qquad [27]$$

Using the boundary conditions $g(1) = n(1) = C$ one finds that $\mathcal{J}_c^{nucl}$ is fully defined by $n(x)$:

$$\mathcal{J}_c^{nucl} = \frac{1}{\sum_{x=1}^{\infty}[P(x)n(x)]^{-1}} \qquad [28]$$

Generally, $n(x)$ has a pronounced minimum at some critical size, $x = x_{cr}$, and the main contribution to the denominator of eqn [28] comes from the clusters with size around x_{cr}. Expanding $n(x)$ in the vicinity of x_{cr} up to the second derivative and replacing the summation by the integration, one finds an equation for $\mathcal{J}_c^{nucl}$, which is equivalent to that for nucleation of second phase precipitate particles.[64,65] Note that eqn [28] describes the cluster nucleation rate quite accurately even in cases where the nucleation stage coexists with the growth which leads to a decrease of the concentration of mobile defects, C. This can be seen from **Figure 2**, in which the results of numerical integration of ME for void nucleation are compared with that given by eqn [28].[73]

In the case of low temperature irradiation, when all vacancy clusters are thermally stable ($C = C_v$ in the case) and only FPs are produced by irradiation,

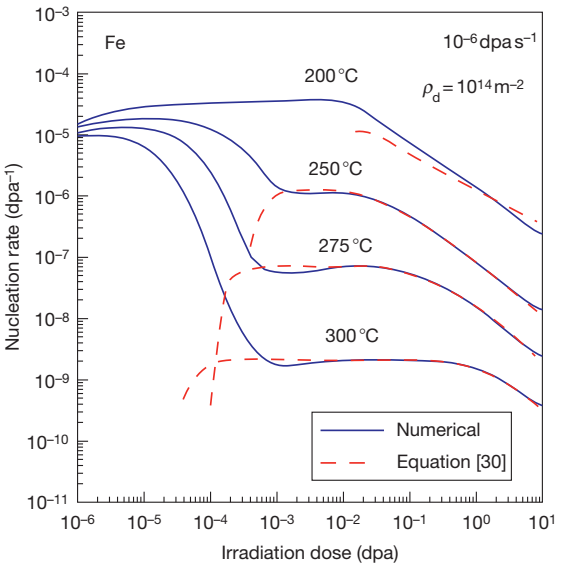

Figure 2 Comparison of the dependences of the void nucleation rate as a function of irradiation dose calculated using master equation, eqns [18] and [28]. From Golubov and Ovcharenko.[73]

the void nucleation rate, eqn [21], can be calculated analytically. Indeed, in the case where the binding energy of a vacancy with voids of all sizes is infinite, $E_v^b(x) = \infty$ (see eqn [75]), it follows from eqn [25] that the function $n(x)$ is equal to

$$n(x) = \frac{C_v}{x^{1/3}}\left(\frac{D_v C_v}{D_i C_i}\right)^{x-1} \quad [29]$$

Substituting eqn [29] in eqn [28], one can easily find that the nucleation rate, $\mathcal{J}_c^{nucl}$, takes the form

$$\mathcal{J}_c^{nucl} = wC_v D_v C_v \frac{1}{\sum_{x=1}^{\infty}\left(\frac{D_i C_i}{D_v C_v}\right)^{x-1}} \quad [30]$$

where $w = (48\pi^2/\Omega^2)^{1/3}$ is a geometrical factor of the order of $10^{20}\,m^{-2}$ (see **Section 1.13.5**). The sum in the dominant eqn [30] is a simple geometrical progression and therefore it is equal to

$$\sum_{x=1}^{\infty}\left(\frac{D_i C_i}{D_v C_v}\right)^{x-1} = \frac{1}{1 - D_i C_i/D_v C_v} \equiv \frac{D_v C_v}{D_v C_v - D_i C_i} \quad [31]$$

Substituting eqn [31] to eqn [30], one can finally obtain the following equation

$$\mathcal{J}_c^{nucl} = wC_v(D_v C_v - D_i C_i) \quad [32]$$

Note that the function $g(x)$ in this case takes a very simple form, $g(x) = C_c/x^{1/3}$, and hence decreases with increasing cluster size. In contrast, in R-space, $g(R)$ (see eqn [16]) increases with increasing cluster size: $g(R) = (36\pi/\Omega)^{1/3} C_c R$ (see also eqns [43] and [44] in Feder *et al.*[69]).

The real time-dependent SDF builds up around the function $g(x)$ with the steadily increasing size range (see, e.g., **Figure 2** in Feder *et al.*[69]). Also note that homogeneous nucleation is the only case where an analytic equation for the nucleation rate exists. In more realistic scenarios, the nucleation is affected by the presence of impurities and other crystal imperfections, and numerical calculations are the only means of investigation. Such calculations are not trivial because for practical purposes it is necessary to consider clusters containing very large numbers of defects and, hence, a large number of equations. This can make the direct numerical solution of ME impractical. As a result several methods have been developed to obtain an approximate numerical solution of ME (see **Section 1.13.4.4** for details).

The equations formulated in this section govern the evolution of mobile and immobile defects in solids under irradiation or aging and provide a framework, which has been used for about 50 years. Application of this framework to the models developed to date is presented in **Sections 1.13.5** and **1.13.6**.

1.13.4.4 Methods of Solving the Master Equation

The ME [18] is a continuity equation (with the source term) for the SDF of defect clusters in a discreet space of their size. This equation provides the most accurate description of cluster evolution in the framework of the mean-field approach describing all possible stages, that is, nucleation, growth, and coarsening of the clusters due to reactions with mobile defects (or solutes) and thermal emission of these same species. The ME is a set of coupled differential equations describing evolution of the clusters of each particular size. It can be used in several ways. For short times, that is, a small number of cluster sizes, the set of equations can be solved numerically.[74] For longer times the relevant physical processes require accounting for clusters containing a very large number of PDs or atoms ($\sim 10^6$ in the case of one-component clusters like voids or dislocation loops and $\sim 10^{12}$ in the case of two-component particles like gas bubbles). Numerical integration of such a system is feasible on modern computers, but such calculations are overly time consuming. Two types of procedures have been developed to deal with this situation: grouping techniques (see, e.g., Feder *et al.*,[69]

Wagner and Kampmann,[70] and Kiritani[75]) and differential equation approximations in continuous space of sizes (see, e.g., Goodrich[67,68], Bondarenko and Konobeev,[76] Ghoniem and Sharafat,[77] Stoller and Odette,[78] Hardouin Duparc *et al.*,[79] Wehner and Wolfer,[80] Ghoniem,[81] and Surh *et al.*[82]). The correspondence between discrete microscopic equations and their continuous limits has been the subject of an enormous amount of theoretical work. The equations of thermodynamics, hydrodynamics, and transport equations, such as the diffusion equation, are all examples of statistically averaged or continuous limits of discrete equations for a large number of particles. The extent to which the two descriptions give equivalent mathematical and physical results has been considered by Clement and Wood.[83] In the following two sections, we briefly discuss these methods.

1.13.4.4.1 Fokker–Plank equation

In the case where the rates $P(x,t), Q(x,t)$ are sufficiently smooth, it is reasonable to approximate them by continuous functions $\tilde{P}(x,t), \tilde{Q}(x,t)$ and to replace the right-hand sides of eqns [18] and [19] by continuous functions of two variables, $\mathcal{J}(x,t)$ and $f(x,t)$. The Fokker–Plank equation can be obtained from the ME by expanding the right-hand side of eqn [18] in Tailor series, omitting derivatives higher than the second order

$$\frac{\partial f^{S}(x,t)}{\partial t} = G^{s}(x) - \frac{\partial}{\partial x}[V(x,t)f(x,t)] + \frac{\partial^2}{\partial x^2}[D(x,t)f(x,t)] \qquad [33]$$

where

$$V(x,t) = \tilde{P}(x,t) - \tilde{Q}(x,t)$$
$$D(x) = \frac{1}{2}[\tilde{P}(x,t) + \tilde{Q}(x,t)] \qquad [34]$$

The first term in eqn [33] describes the hydrodynamic-like flow of clusters, whereas the second term accounts for their diffusion in the size-space. Note that for clusters of large enough sizes, when the cluster evolution is mainly driven by the hydrodynamic term, the functions $\tilde{P}(x,t), \tilde{Q}(x,t)$ are smooth; hence the ME and F–P equations are equally accurate. For sufficiently small cluster sizes, when the diffusion term plays a leading role, eqn [33]) provides only poor description.[67,68,83] As the cluster nucleation normally takes place at the beginning of irradiation, that is, when the clusters are small, the results obtained using F–P equation are expected to be less accurate compared to that of ME.

1.13.4.4.2 Mean-size approximation

In eqn [24], the term with $V(x,t)$ is responsible for an increase of the mean cluster size, while the term with $D(x)$ is responsible for cluster nucleation and broadening of the SDF. For large mean cluster size, most of the clusters are stable and the diffusion term is negligible. This is the case when the nucleation stage is over, and the cluster density does not change significantly with time. A reasonably accurate description of the cluster evolution is then given in the mean-size approximation, when $f_c(x,t) = N_c\delta(x - \langle x(t)\rangle)$ where $\delta(\xi)$ is the Kronecker delta and N_c is the cluster density. The rate of change of the mean size in this case can be calculated by omitting the last term in the right-hand side of eqn [24], multiplying both sides by x, integrating over x from 0 to infinity, and taking into account that $f(x=\infty,t) = 0$ and $f(x=0,t) = 0$

$$\frac{d\langle x\rangle}{dt} = V(\langle x\rangle, t) \qquad [35]$$

1.13.4.4.3 Numerical integration of the kinetics equations

The main idea of the grouping methods for numerical evaluation of the ME is to replace a group of equations described by the ME with an 'averaged' equation. Such a procedure was proposed by Kiritani[75] for describing the evolution of vacancy loops during aging of quenched metals. Koiwa[84] was the first to examine the Kiritani method by comparing numerical results with the results of an analytical solution for a simple problem. Serious disagreement was found between the numerical and analytical results, raising strong doubts regarding the applicability of the method. The main objection to the method[75] in Koiwa[84] is the assumption used by Kiritani[75] that the SDF within a group does not depend on the size of clusters. However, Koiwa did not provide an explanation of where the inaccuracy comes from. The Validity of the Kiritani method was examined thoroughly by Golubov *et al.*[85] The general conclusion of the analysis is that the grouping method proposed by Kiritani is not accurate. The origin of the error is the approximation that the SDF within a group is constant as was predicted by Koiwa.[84] Thus, the disagreement found in Koiwa[84] is fundamental and cannot be circumvented. Because it is important for understanding the accuracy of the other methods suggested for numerical calculations of cluster evolution,

the analysis performed in Golubov *et al.*[85] is briefly highlighted below.

It follows from eqn [18] that the total number of clusters, $N(t) = \sum_{x=2}^{\infty} f(x,t)$ and total number of defects in the clusters, $S(t) = \sum_{x=2}^{\infty} xf(x,t)$, are described by the following equations:

$$\frac{\partial N}{\partial t} = \mathcal{J}(1,t) \quad [36]$$

$$\frac{\partial S}{\partial t} = \mathcal{J}(1,t) + \sum_{x=1}^{\infty} \mathcal{J}(x,t) \quad [37]$$

where the generation term in eqn [18] is dropped for simplicity. Equations [36] and [37] are the conservation laws which can be satisfied when one uses a numerical evaluation of the ME. When a group method is used, the conservation laws can be satisfied for reactions taking place within each group.[69] However, this is not possible within the approximation used by Kiritani[75] because a single constant can be used to satisfy only one of the eqns [36] and [37]. To resolve the issue, Kiritani[75] used an ad hoc modification of the flux $\mathcal{J}(x_i)$; therefore, the final set of equations for the density of clusters within a group, F_i, are as follows

$$\frac{\mathrm{d}F_i}{\mathrm{d}t} = \frac{1}{\Delta x_i}[\mathcal{J}_{i-1} - \mathcal{J}_i] \quad [38]$$

$$\mathcal{J}_i = \frac{2\Delta x_i}{\Delta x_i + \Delta x_{i+1}} P_i F_i - \frac{2\Delta x_{i+1}}{\Delta x_i + \Delta x_{i+1}} Q_{i+1} F_{i+1} \quad [39]$$

where Δx_i is the width of the 'i' group. Equations [38] and [39] indeed satisfy both the conservation laws. However, they do not provide a correct description of cluster evolution described by the ME because the flux $\mathcal{J}_i$ in eqn [39] depends on the widths of groups and these widths have no physical meaning. An example of a comparison of the calculation results obtained using the Kiritani method with the analytical and numerical calculations based on a more precise grouping method is presented in **Figure 3**. Note that in the limiting case where the widths of group are equal, $\Delta x_i = \Delta x_{i+1}$, the flux $\mathcal{J}_i$ is equal to the original one, $\mathcal{J}(x,t)$. In this limiting case, eqns [38] and [39] correspond to those that can be obtained by a summation of the ME within a group and therefore they provide conservation of the total number of clusters, $N(t)$, only. This limiting case is probably the simplest way to demonstrate the inaccuracy of the Kiritani method.

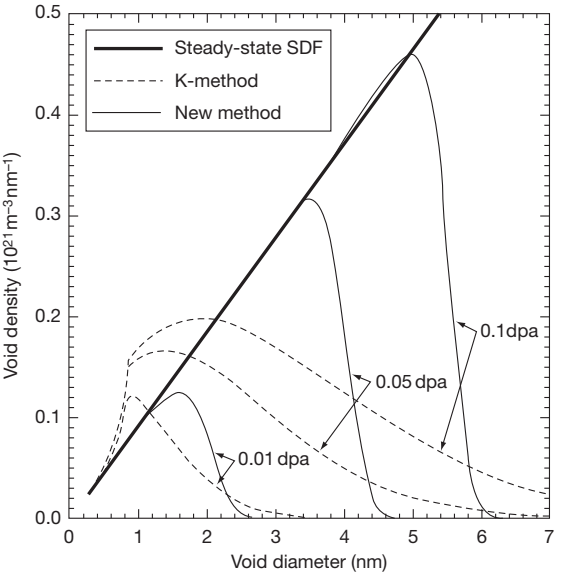

Figure 3 Size distribution function of voids calculated in copper irradiated at 523 K with the damage rate of 10^{-7} dpa s^{-1} for doses of 10^{-2}–10^{-1} dpa. The dashed and solid lines correspond to the Kiritani method and the new grouping method, respectively. The thick line corresponds to the steady-state function, $g(x)$. Reproduced from Golubov, S. I.; Ovcharenko, A. M.; Barashev, A. V.; Singh, B. N. *Philos. Mag. A* **2001**, *81*, 643–658.

It is worth noting that this comparison also sheds light on the relative accuracy of other numerical solutions of the F–P equation such as in Bondarenko and Konobeev,[76] Ghoniem and Sharafat,[77] Stoller and Odette,[78] and Hardouin Duparc *et al.*[79]

Equations [36] and [37] provide a way of getting a simple but still reasonably correct grouping method for numerical integration of the ME. Indeed, the two conservation laws, eqns [36] and [37], require two parameters within a group at least. The simplest approximation of the SDF within a group of clusters (sizes from x_{i-1} to $x_i = x_{i-1} + \Delta x_i - 1$) can be achieved using a linear function

$$f_i(x) = L_0^i(x - \langle x \rangle_i) + L_1^i \quad [40]$$

where $\langle x \rangle_i = x_i - 1/2(\Delta x_i - 1)$ is the mean size of the group. Equations for L_0^i, L_1^i are as follows[69]

$$\frac{\mathrm{d}L_0^i}{\mathrm{d}t} = \frac{1}{\Delta x_i}[\mathcal{J}(x_{i-1}) - \mathcal{J}_x(x_i)] \quad [41]$$

$$\frac{\mathrm{d}L_1^i}{\mathrm{d}t} = -\left(\frac{\Delta x_i - 1}{2\sigma_i^2 \Delta x_i}\right)\left\{\mathcal{J}_x(x_{i-1}) + \mathcal{J}(x_i) - 2\mathcal{J}\left(\langle x_i \rangle - \frac{1}{2}\right)\right\} \quad [42]$$

where

$$\sigma_i^2 = \frac{1}{\Delta x_i}\left[\sum_{k=x_{i-1}+1}^{x_i} k^2 - \frac{1}{\Delta x_i}\left(\sum_{k=x_{i-1}+1}^{x_i} k\right)^2\right] \qquad [43]$$

is the dispersion of the group. Equations [41] and [42] describe the evolution of the SDF within the group approximation. Note that the last term in the brackets on the right-hand side of eqn [42] follows from the corresponding term in eqn [38] in Golubov *et al.*[85] when the rates $P(x,t), Q(x,t)$ are independent from x within the group. Note also that the factor '$-1/\Delta x_i$' is missing in eqn [38] in Golubov *et al.*[85]

As can be seen from eqns [41] and [42], in the case where $\Delta x_i = 1$, eqns [41] and [42] transform to eqn [18], that is $f(x_i) = L_0^i$ and $L_1^i = 0$ in contrast with Kiritani's method, where the equation describing the interface number density of clusters between ungrouped and grouped ones has a special form (see, e.g., eqn [21] in Koiwa[84]). It has to be emphasized that this grouping method is the only one that has demonstrated high accuracy in reproducing well-known analytical results such as those by Lifshitz–Slezov–Wagner[86,87] (LSW) and Greenwood and Speight[88] describing the asymptotic behavior of SDF in the case of secondary phase particle evolution[89] and gas bubble evolution[90] during aging.

A different approach for calculating the evolution of the defect cluster SDF is based on the use of the F–P equation. Note that the use of eqn [33] as an approximate method for treating cluster evolution is not new, for the work initiated by Becker and Döring[64] has been brought into its modern form by Frenkel.[66] An advantage of the F–P equation over the ME is based on the possibility of using the differential equation methods developed for the case of continuous space. Quite comprehensive applications of the analytical methods to solve the F–P have been done by Clement and Wood.[83] It has been shown[83] that convenient analytical solutions of the F–P equation cannot be obtained for the interesting practical cases. Thus, several methods have been suggested for an approximate numerical solution for it. The simplest method is based on discretization of the F–P equation[76–79] that transforms it to a set of equations for the clusters of specific sizes similar to the ME; in both the cases the matrix of coefficients of the equation set is trigonal. This method is convenient for numerical calculations and allows calculating cluster evolution up to very large cluster sizes (e.g., Ghoniem[81]). However, this method is not accurate because it is identical to the approach used by Kiritani[75] in which SDF was approximated by a constant within a group. Thus, all the objections to Kiritani's method discussed above are valid for this method as well. Also note that the method has a logic problem. Indeed a chain of mathematical transformations, namely ME to F–P and F–P to discretized F–P, results in a set of equations of the same type, which can be obtained by simple summation of ME within a group. Moreover, the last equation is more accurate compared to the discretized F–P because it is a reduced form of the ME.

Another approach for numerical integration of the F–P equation was suggested by Wehner and Wolfer (see Wehner and Wolfer[80]). The method allows calculating cluster evolution on the basis of a numerical path-integral solution of the F–P equation which provides an exact solution in the limiting case where the time step of integration approaches zero. For a finite time step, the method provides an approximate solution with an accuracy that has not been verified. Moreover, there was an error in the calculation presented in Wehner and Wolfer[80,91] and so the accuracy of the method remains unclear. A modification of this method according to which the evolution of large clusters is calculated by employing a Langevin Monte Carlo scheme instead of the path integral was suggested by Surh *et al.*[82] The accuracy of this method has not been verified as an error was also made in obtaining the results presented in Surh *et al.*[82,91]

The momentum method for the solution of the F–P equation used by Ghoniem[81] (see also Clement and Wood[83]) is quite complicated and may provide only an approximate solution. So far, none of the methods suggested for numerical evaluation of the F–P equation has been developed and verified to a sufficient degree to allow effective and accurate calculations of defect cluster evolution during irradiation in the practical range of doses and temperatures.

1.13.5 Early Radiation Damage Theory Model

The chemical reaction RT was used very early to model the damage accumulation under irradiation (Brailsford and Bullough[92] and Wiedersich[93]). The main assumptions were as follows: (1) the incident irradiation produces isolated FPs, that is, single SIAs and vacancies in equal numbers, (2) both SIAs and vacancies migrate 3D, and (3) the efficiencies of the SIAs and vacancy absorption by different sinks are different because of the differences in the strength of

the corresponding PD-sink elastic interactions. Thus, the preferential absorption of SIAs by dislocations (i.e., the dislocation bias) is the only driving force for microstructural evolution in this model, which is a variant of the FP3DM. It should be emphasized that, in the framework of the FP3DM, no distinction is made between different types of irradiation: ~1 MeV electrons, fission neutrons, and heavy-ions. It was believed that the initial damage is produced in the form of FPs in all these cases. Now we understand the mechanisms operating under different conditions much better and make clear distinction between electron and neutron/heavy-ion irradiations (see Singh *et al.*,[1,22] Garner *et al.*,[33] Barashev and Golubov,[35] and references therein for some recent advances in the development of the so-called PBM). However, the FP3DM is the simplest model for damage production and it correctly describes 1 MeV electron irradiation. It is therefore useful to consider it first. The more comprehensive PBM includes the FP3DM as its limiting case.

1.13.5.1 Reaction Kinetics of Three-Dimensionally Migrating Defects

In the case considered, eqns [10]–[12] for mobile defects are reduced to the following form

$$\frac{dC_v}{dt} = G^{NRT} + G_v^{th} - k_v^2 D_v C_v - \mu_R D_i C_i C_v$$
$$\frac{dC_i}{dt} = G^{NRT} - k_i^2 D_i C_i - \mu_R D_i C_i C_v \qquad [44]$$

In order to predict the evolution of mobile PDs and their impact on immobile defects, one needs to know the sink strength of different defects for vacancies and SIAs and the rate of their mutual recombination. The reaction kinetics of 3D migrating defects is considered to be of the second order because the rate equations contain terms with defect concentrations to the second power.[40] An important property of such kinetics is that the leading term in the sink strength of any individual defect depends on the characteristics of this defect only. Thus,

$$k_\alpha^2 = \sum_{j=1}^{N} k_{\alpha j}^2 \qquad [45]$$

where $\alpha = v, i$ and N is the total number of sinks per unit volume. For example, the total sink strength of an ensemble of voids of the same radius, R, is equal to $k_\alpha^2 = N k_\alpha^2(R)$. The individual sink strength such as a void or a dislocation loop may be obtained from a solution to the PD diffusion equation. In the following section, we present examples of such a treatment based on the so-called lossy-medium approximation.[61]

1.13.5.1.1 Sink strength of voids

Consider 3D diffusion of mobile defects near a spherical cavity of radius R, which is embedded in a lossy-medium of the sink strength k^2:

$$G - k^2 D(C - C^{eq}) - \nabla \mathcal{J} = 0 \qquad [46]$$

where C^{eq} is the thermal-equilibrium concentration of mobile defects and the defect flux is

$$\mathcal{J} = -D\left(\nabla C + \frac{C}{k_B T}\nabla U\right) \qquad [47]$$

Here, D is the diffusion coefficient, U is the interaction energy of the defect with the void, k_B is the Boltzmann constant, and T the absolute temperature. The boundary conditions for the defect concentration, C, at the void surface and at infinity are

$$C(R) = C^{eq} \qquad [48]$$

$$C^{\infty} = C^{eq} + \frac{G}{k^2 D} \qquad [49]$$

Equation [49] follows from eqn [46] and the requirement that the gradients vanish at large distances. Here, all other sinks in the system, voids, dislocations, etc. are considered in the MFA and contribute to the total sink strength k^2. This procedure is self-consistent.

The interaction energy of a defect with the void in eqn [47] is small and usually neglected. The solution of eqn [46] for a void located at the origin of the coordinate system, $r = 0$, is then

$$C(r) = C^{eq} + (C^{\infty} - C^{eq})\left\{1 - \frac{R}{r}\exp[-k(r-R)]\right\} \qquad [50]$$

The total defect flux, I, through the void surface $S = 4\pi R^2$ is given by

$$I = -S\mathcal{J}(R) = k_C^2(R) D(C^{\infty} - C^{eq}) \qquad [51]$$

where the void sink strength is

$$k_C^2(R) = 4\pi R(1 + kR) \qquad [52]$$

The sink strength of all voids in the system is obtained by integrating over the SDF, $f(R)$:

$$k_C^2 = \int dR k_C^2(R) f(R) = 4\pi \langle R \rangle N_C \left(1 + k\frac{\langle R^2 \rangle}{\langle R \rangle}\right) \qquad [53]$$

where $N_C = \int dR f(R)$ is the void number density, $\langle R \rangle$ is the void mean radius and $\langle R^2 \rangle$ is the mean radius squared. Typically, $k^2 \approx 10^{14} m^{-2}$, that is,

$k^{-1} \approx 100$ nm, while the void radii are much smaller, so that one can omit the term proportional to the radius squared:

$$k_C^2 = 4\pi\langle R\rangle N_C \qquad [54]$$

Equation [52] is derived by neglecting the interaction between the void and mobile defect. There is a difference between the interaction of SIAs and vacancies with voids due to differences in the corresponding dilatation volumes. As a result, the void capture radius for an SIA is slightly larger than that for a vacancy (see, e.g., Golubov and Minashin[94]). However, this difference is usually negligible compared to that for an edge dislocation, which is described below.

1.13.5.1.2 Sink strength of dislocations

An equation for the dislocation sink strength can be derived the same way as for voids. In this case, eqn [46] is solved in a cylindrical coordinate system and the interaction between PDs and dislocation is significant and not omitted. For an elastically isotropic crystal and PDs in the form of spherical inclusions, the interaction energy has the form[95]

$$U(r,\theta) = -\frac{A\sin\theta}{r} \qquad [55]$$

where

$$A = \frac{\mu b}{3\pi}\frac{1+\nu}{1-\nu}\Delta\Omega \qquad [56]$$

μ is the shear modulus, ν the Poisson ratio and $\Delta\Omega$ the dilatation volume of the PD under consideration. The solution of eqn [35] in this case was obtained by Ham[95] but is not reproduced here because of its complexity. It has been shown that a reasonably accurate approximation is obtained by treating the dislocation as an absorbing cylinder with radius $R_d = Ae^{\gamma}/4k_BT$, where $\gamma = 0.5772$ is Euler's constant.[95] The solution is then given by

$$C(r) = \frac{G}{Dk^2}\left[1 - \frac{K_0(kr)}{K_0(kR_d)}\right] \qquad [57]$$

where $K_0(x)$ is the modified Bessel function of zero order. Using eqns [47] and [57], one obtains the total flux of PDs to a dislocation and the dislocation sink strength as

$$I = -2\pi R_d\rho_d D\mathcal{J}(R_d) = k_d^2 D(C^{\infty} - C^{eq}) \qquad [58]$$

$$k_d^2 = \rho_d Z^d$$
$$Z^d = \frac{2\pi}{\ln(1/kR_d)} \qquad [59]$$

where ρ_d is the dislocation density and Z^d the capture efficiency. The capture efficiencies for vacancies and SIAs, Z_v^d and Z_i^d, are different because of the difference in their dilatation volumes (see eqn [56])

$$Z_\alpha^d = \frac{2\pi}{\ln(1/kR_d^\alpha)} \qquad [60]$$

where $\alpha = v, i$ and

$$R_d^\alpha = \frac{\mu b}{3\pi}\frac{1+\nu}{1-\nu}\left(\frac{e^\gamma}{4k_BT}\right)\Delta\Omega_\alpha \qquad [61]$$

The dilatation volume of SIAs is larger than that of vacancies, hence $R_D^i > R_D^v$ and the absorption rate of dislocations is higher for SIAs: $Z_i^d > Z_v^d$. This is the reason for void swelling, which is shown below in Section 1.13.5.2.1. A more detailed analysis of the sink strengths of dislocations and voids for 3D diffusing PDs can be found in a recent paper by Wolfer.[96]

1.13.5.1.3 Sink strengths of other defects

The sink strengths of other defects can be obtained in a similar way. For dislocation loops of a toroidal shape[97]

$$k_{L(v,i)}^2 = 2\pi R_L Z_L^{v,i}$$
$$Z_L^{v,i} = \frac{2\pi}{\ln(8R_L/r_{core}^{v,i})} \qquad [62]$$

where R_L and $r_{core}^{v,i}$ are the loop radius and the effective core radii for absorption of vacancies and SIAs, respectively. Similar to dislocations, the capture efficiency for SIAs is larger than that of vacancies, $Z_L^i > Z_L^v$, for loops.

For a spherical GB of radius R_G (see, e.g., Singh *et al.*[98])

$$k_{GB}^2 = \frac{1}{R_G^2}\frac{3\xi^2(\xi\coth\xi - 1)}{\xi^2 - 3(\xi\coth\xi - 1)} \qquad [63]$$

where $\xi = kR_G$. In the limiting case of $\xi \ll 1$, that is, when the GB is the main sink in the system,

$$k_{GB}^2 = \frac{15}{R_G^2} \qquad [64]$$

For the surfaces of a thin foil of thickness L (see eqn [7] in Golubov[99])

$$k_{foil}^2 = \frac{k^2}{kL/2\coth(kL/2) - 1} \qquad [65]$$

In the limiting case of $kL \ll 1$, that is, when the foil surfaces are the main sinks,

$$k_{foil}^2 = \frac{12}{L^2} \qquad [66]$$

1.13.5.1.4 Recombination constant

Equation [35] can be used to obtain the rate of recombination reactions between vacancies and SIAs. In a coordinate system where the vacancy is immobile, the SIAs migrate with the diffusion coefficient $D_i + D_v$ and, hence, the total recombination rate is

$$R = 4\pi r_{\text{eff}}(D_i + D_v)C_i n_v \approx \mu_R D_i C_i C_v \qquad [67]$$

where $n_v = C_v/\Omega$ and the fact that $D_i \gg D_v$ at any temperature is used. In this equation, r_{eff} is the effective capture radius of a vacancy, defining an effective volume where recombination occurs spontaneously (athermally). The recombination constant, μ_R, in eqn [67] is, hence, equal to

$$\mu_R \approx \frac{4\pi r_{\text{eff}}}{\Omega} \qquad [68]$$

MD calculations show that a region around a vacancy, where such a spontaneous recombination takes place, consists of ~100 lattice sites.[100,101] From $4\pi r_{\text{eff}}^3/3 = 100\Omega$, one finds that r_{eff} is approximately two lattice parameters, hence $\mu_R \approx 10^{21}\,\text{m}^{-2}$.

1.13.5.1.5 Dissociation rate

Dissociation of vacancies from voids and other defects is an important process, which significantly affects their evolution under irradiation and during aging. Similar to the absorption rate eqn [54], it has been shown that the dissociation rate is proportional to the void radius. Such a result can readily be obtained by using the so-called detailed balance condition. However, as the evaporation takes place from the void surface, the frequency of emission events is proportional to the radius squared. In the following lines, we clarify why the dissociation rate is proportional to the void radius and elucidate how diffusion operates in this case.

Consider a void of radius R, which emits $\nu_{\text{diss}} = \tau_{\text{diss}}^{-1}$ vacancies per second per surface site in a spherical coordinate system. Vacancies migrate 3D with the diffusion coefficient $D_v = a^2/6\tau$, where a is the vacancy jump distance and τ is the mean time delay before a jump. The diffusion equation for the vacancy concentration C_v is

$$\nabla^2 C_v = 0 \qquad [69]$$

To calculate the number of vacancies emitted from the void and reach some distance R^∞ from the void surface, we use absorbing boundary conditions at this distance

$$C_v(R^\infty) = 0 \qquad [70]$$

An additional boundary condition must specify the vacancy–void interaction. Assuming that vacancies are absorbed by the void, which is a realistic scenario, the vacancy concentration at one jump distance a from the surface can be written as

$$\frac{C_v(R+a)}{\tau} = \nu_{\text{diss}} + \frac{C_v(R+2a)}{2\tau} \qquad [71]$$

The left-hand side of the equation describes the frequency with which vacancies leave the site. The first term on the right-hand side accounts for the production of vacancies due to evaporation from the void. The last term on the right-hand side accounts for vacancies coming to this site from sites further way from the void surface. After representing the latter term using a Taylor series, in the limit of $R \gg a$, the boundary condition, eqn [71], assumes the following form

$$C_v(R) = 2\tau\nu_{\text{diss}} + a\nabla C_v(R) \qquad [72]$$

Using this condition and eqns [69] and [70], one finds the vacancy concentration, $C_v(r)$, is equal to

$$C_v(r) = 2\tau\nu_{\text{diss}}\frac{r^{-1} - (R^\infty)^{-1}}{R^{-1} - (R^\infty)^{-1}} \qquad [73]$$

It can readily be estimated using the last two equations that the gradient of concentration in eqn [72] is smaller than the other terms by a factor of a/r_0 and does not contribute to eqn [73]. This means that most vacancies emitted from the void return to it. As a result, the equilibrium condition for the concentration near the void surface is defined by the equality of the frequency of evaporation and the frequency of jumps back to the surface and is not affected by the flux of vacancies away from the surface. The vacancy equilibrium concentration at the void surface is readily obtained from eqn [73] as $C_v^{\text{eq}}(R) = C_v(R) = 2\tau\nu_{\text{diss}}$.

The total number of vacancies passing through a spherical surface of radius R and area $S = 4\pi R^2$ per unit time, that is, the rate of vacancy emission from the void, is equal to

$$\mathcal{J}_v^{\text{em}} = -\frac{SD_v}{\Omega}\nabla C_v(r)_{|r=R} = \frac{D_v C_v^{\text{eq}}}{\Omega}\frac{4\pi R}{1 - R/R^\infty} \approx \frac{D_v C_v^{\text{eq}}}{\Omega}4\pi R \qquad [74]$$

There are three points to be made. First, eqn [73] becomes independent of the distance r from the surface, when $r \gg R$. Thus, vacancies reaching this distance are effectively independent of their origin and can be counted as dissociated from the void. Second, despite the fact that the total vacancy

emission frequency is proportional to the void surface area, the total vacancy flux far away from the surface is proportional to the void radius. This is a well-known result of the reaction–diffusion theory[40] considering the void capture efficiency. Third, as can be seen from eqn [74], significant deviation from the proportionality to the void radius occurs at distances of the order of the void radius.

As discussed above, most emitted vacancies return to the void. The fraction of vacancies which do not return is equal to the ratio of the frequency defined by eqn [63] and the total frequency of vacancy emission $\sim 4\pi R^2 v_{\mathrm{diss}}/a^2$. It is thus equal to a/R. The same result can be demonstrated considering another, although unrealistic, scenario in which vacancies are reflected by the voids.[102] We also note that the first nonvanishing correction to the proportionality of the vacancy flux to the void radius is positive and proportional to the void radius squared, see eqn [74], where $R(1-R/R^{\infty})^{-1} \approx R + R^2/R^{\infty}$. The same result was obtained previously by Gösele[40] when considering void capture efficiency. Thus, with increasing volume fraction more and more vacancies become absorbed at other voids and the proportionality to the void radius squared would be restored. The first correction term just shows the right tendency.

1.13.5.1.6 Void growth rate

The concentration of vacancies in equilibrium with a void of radius R, $C_{\mathrm{v}}^{\mathrm{eq}}(R)$, which enters eqn [74], can be obtained by considering the free energy of a crystal with a void and a solution of vacancies. Let x be the number of vacancies taken from a solution of vacancies to make a spherical void of a radius $R = (3x\Omega/4\pi)^{1/3}$. The associated free energy change is given by

$$\Delta F = -\left(\frac{4\pi R^3}{3\Omega}\right)\mu_{\mathrm{v}} + 4\pi\tilde{\gamma}R^2 \qquad [75]$$

where $\mu_{\mathrm{v}} = k_{\mathrm{B}}T\ln\left(C_{\mathrm{v}}/C_{\mathrm{v}}^{\mathrm{th}}\right)$ is the chemical potential of a vacancy ($C_{\mathrm{v}}^{\mathrm{th}}$ is the equilibrium concentration in a perfect crystal) and $\tilde{\gamma}$ is the void surface energy. By differentiating this equation with respect to radius and equating the result to zero, one can find the equilibrium vacancy concentration, which is given by

$$C_{\mathrm{v}}^{\mathrm{eq}}(R) = C_{\mathrm{v}}^{\mathrm{th}}\exp\left(\frac{2\Omega\tilde{\gamma}}{Rk_{\mathrm{B}}T}\right) \qquad [76]$$

Absorption and emission of PDs change a void volume on the basis of the flux of PDs $\mathrm{d}\Delta V/\mathrm{d}t = 4\pi R^2(\mathrm{d}R/\mathrm{d}t) = (\mathcal{J}_{\mathrm{v}} - \mathcal{J}_{\mathrm{i}} - \mathcal{J}_{\mathrm{v}}^{\mathrm{em}})$. With the aid of eqns [51], [52], [74] and keeping the leading term proportional to R only and [76], the growth rate of a void due to absorption of vacancies and SIAs and vacancy emission can be written as

$$\frac{\mathrm{d}R}{\mathrm{d}t} = \frac{1}{R}\left[D_{\mathrm{v}}C_{\mathrm{v}} - D_{\mathrm{i}}C_{\mathrm{i}} - D_{\mathrm{v}}C_{\mathrm{v}}^{\mathrm{th}}\exp\left(\frac{2\Omega\tilde{\gamma}}{Rk_{\mathrm{B}}T}\right)\right] \qquad [77]$$

Neglecting the entropy factor for simplicity, one can find that $C_{\mathrm{v}}^{\mathrm{th}} = \exp(-E_{\mathrm{v}}^{\mathrm{f}}/k_{\mathrm{B}}T)$, where $E_{\mathrm{v}}^{\mathrm{f}}$ is the vacancy formation energy. The last term in the square brackets on the right-hand side of eqn [66] can be then represented in the following form

$$D_{\mathrm{v}}C_{\mathrm{v}}^{\mathrm{th}}\exp\left(\frac{2\Omega\tilde{\gamma}}{Rk_{\mathrm{B}}T}\right) \equiv D_{\mathrm{v}}\exp\left(-\frac{E_{\mathrm{b}}}{Rk_{\mathrm{B}}T}\right) \qquad [78]$$

where

$$E_{\mathrm{b}} = E_{\mathrm{v}}^{\mathrm{f}} - \frac{2\Omega\tilde{\gamma}}{R} \qquad [79]$$

is a well-known equation for the binding energy of a vacancy with a void that is valid for large enough radius. For voids of small sizes, the value E_{b} has to be calculated by using *ab initio* or MD methods.

Equation [77] is used in calculations of void swelling. Note that the vacancy and SIA fluxes, the first and second terms, enter this equation symmetrically and this is because of the neglect of the difference in the interactions of SIAs and vacancies with voids. Also, when the sum of the second and third terms in the right-hand side of this equation is larger than the first term, the voids shrink. Such a shrinking takes place during annealing of preirradiated samples or, in some cases, during irradiation, if the irradiation conditions are changed. However, in the majority of cases, voids grow under irradiation because dislocations interact more strongly with SIAs than vacancies.

1.13.5.1.7 Dislocation loop growth rate

The concentration of vacancies, $(C_{\mathrm{v}}^{\mathrm{eq}})_{\mathrm{vl,il}}$, in equilibrium with the dislocation loop of radius R of vacancy (subscript 'vl') and SIA (subscript 'il') type can be obtained in the same way as in the previous subsection (e.g., Bullough *et al.*[29])

$$(C_{\mathrm{v}}^{\mathrm{eq}})_{\mathrm{vl,il}} = C_{\mathrm{v}}^{\mathrm{th}}\exp\left(\pm\frac{(\gamma_{\mathrm{sf}} + E_{\mathrm{el}})b^2}{k_{\mathrm{B}}T}\right) \qquad [80]$$

where γ_{sf}, E_{el}, and b are the stacking-fault energy, the interaction energy of PDs with dislocation and the dislocation Burgers vector, respectively. The '+' and '−' in the exponent correspond to the cases of vacancy and SIA loops, respectively. In the case

when both PDs are considered as spherical dilation centers, the interaction energy E_{el} is given by

$$E_{el} = \frac{\mu b^2}{4\pi(1-\nu)(R+b)} \ln\left(\frac{R+b}{b}\right) \quad [81]$$

where μ and ν are the shear modulus and Poisson ratio, respectively. Hence, the growth rates of vacancy and SIA loops are

$$\frac{dR_{vl}}{dt} = \frac{1}{b}\left[Z_L^v D_v C_v - Z_L^i D_i C_i - Z_L^v D_v C_v^{th} \exp\left(\frac{(\gamma_{sf}+E_{el})b^2}{k_B T}\right)\right]$$

$$\frac{dR_{il}}{dt} = \frac{1}{b}\left[Z_L^i D_i C_i - Z_L^v D_v C_v + Z_L^v D_v C_v^{th} \exp\left(-\frac{(\gamma_{sf}+E_{el})b^2}{k_B T}\right)\right] \quad [82]$$

1.13.5.1.8 The rates P(x) and Q(x)

Equations [54] and [62] for the sink strengths of voids and dislocation loops for mobile PDs permit the calculation of rates $P(x)$ and $Q(x)$, which determine the cluster evolution described by the ME (see **Section 1.13.4.3.2**). For example, the total rate of absorption of vacancies by voids is equal to $k_c^2 D_v C_v$ (see eqns [10] and [45]). The same quantity is given by $\sum_{x=2}^{\infty} P_c(x) f_c(x)$. By equating these two rates one obtains

$$D_v C_v k_c^2 = \sum_{x=2}^{\infty} P_c(x) f_c(x) \quad [83]$$

Taking into account eqns [14] and [54], the following expression for the rate $P_c(x)$ can readily be obtained

$$P_c(x) = w_c x^{1/3} D_v C_v \quad [84]$$

where

$$w_c = \left(\frac{48\pi^2}{\Omega^2}\right)^{1/3} \quad [85]$$

The rate $Q_c(x)$, which consists of two terms, the SIA absorption and vacancy emission rates, can be obtained the same way

$$Q_c(x) = w_c x^{1/3}\left[D_i C_i + D_v \exp\left(\frac{-E_v^b(x)}{k_B T}\right)\right] \quad [86]$$

For dislocation loops of SIA type, the rates $P_{il}(x)$ and $Q_{il}(x)$ take the following form

$$P_{il}(x) = w_l x^{1/2}\left[Z_L^i D_i C_i + Z_L^v D_v \exp\left(\frac{-E_{il}^b(x)}{k_B T}\right)\right]$$

$$Q_{il}(x) = w_l x^{1/2} Z_L^v D_v C_v \quad [87]$$

where

$$w_l = \left(\frac{4\pi}{\Omega b}\right)^{1/2}$$

$$E_{il}^b(x) = E_v^f + (\gamma_{sf} + E_{el}(x))b^2 \quad [88]$$

For vacancy loops, the rates $P_{vl}(x)$ and $Q_{vl}(x)$ are given by

$$P_{vl}(x) = w_l x^{1/2} Z_L^i D_v C_v$$

$$Q_{vl}(x) = w_l x^{1/2}\left[Z_L^i D_i C_i + Z_L^v D_v \exp\left(\frac{-E_{vl}^b(x)}{k_B T}\right)\right] \quad [89]$$

where

$$E_{il}^b(x) = E_v^f - [\gamma_{sf} + E_{el}(R)]b^2 \quad [90]$$

The equations given above have been obtained by neglecting mutual recombination between vacancies and SIAs. Accounting for recombination makes the diffusion equations for the concentrations of PDs nonlinear, an approximate solution for which has been obtained using a linearization procedure.[103] The correction is, however, insignificant for conditions of practical importance.

1.13.5.2 Damage Accumulation

Damage accumulation in pure metals during irradiation primarily takes place in the formation and evolution of vacancy and SIA-type defects. At temperatures higher than recovery stage III, which is the main interest for practical purposes, vacancy clusters normally take the form of voids that result in the change of a volume, that is, swelling. Owing to limitations of space, in the following section we focus only on a description of void evolution.

1.13.5.2.1 Void swelling

The solution obtained from eqns [44] depends on the irradiation temperature. Temperatures below recovery stage II will not be considered here. At temperatures smaller than that corresponding to the recovery stage III, when vacancies are immobile and the interstitials are mobile, the concentration of vacancies will build up. At some irradiation dose, the vacancy concentration will become high enough that mutual recombination of PDs may become the dominant mechanism of the defect loss, thus controlling defect accumulation. In this case,

the dose dependence of PD concentrations can be calculated analytically[104]

$$D_i C_i(t) = \left(\frac{G^{NRT}}{2\mu_R}\right)^{1/2} \left[\int_0^t k^2(\tau)\mathrm{d}\tau\right]^{-1/2}$$

$$D_v C_v(t) = \left(\frac{G^{NRT}}{2\mu_R}\right)^{1/2} \int_0^t k^2(\tau) \left[\int_0^\tau k^2(\tau_1)\mathrm{d}\tau_1\right]^{-1/2} \mathrm{d}\tau \quad [91]$$

Because the sink strength, $k^2(\tau)$, changes very slowly (the vacancy-type defects shrink and SIA-type defects grow because of the SIA absorption), it follows from eqn [91] that

$$D_i C_i(t) \propto (G^{NRT} t)^{-1/2}$$
$$D_v C_v(t) \propto (G^{NRT} t)^{1/2} \quad [92]$$

At temperatures higher than that corresponding to recovery stage III, both vacancies and SIAs are mobile. Hence, after a certain time of irradiation, called the 'transient period', their concentrations reach a steady state. A comprehensive analysis of the time (irradiation dose) dependence of PD concentrations for different sink strength can be found in Sizmann.[9] The dose dependence of PD concentrations and void swelling obtained by the numerical integration of ME[73] is presented in **Figure 4**. As can be seen, the vacancy supersaturation, $(D_v C_v - D_i C_i)/D_v C_v^{eq}$, becomes positive when the PD concentrations reach steady state and this gives rise to void growth. Also, note that in the transient regime only divacancies are formed. In the following discussion we concentrate on the irradiation doses beyond the transient period, which are of more practical interest.

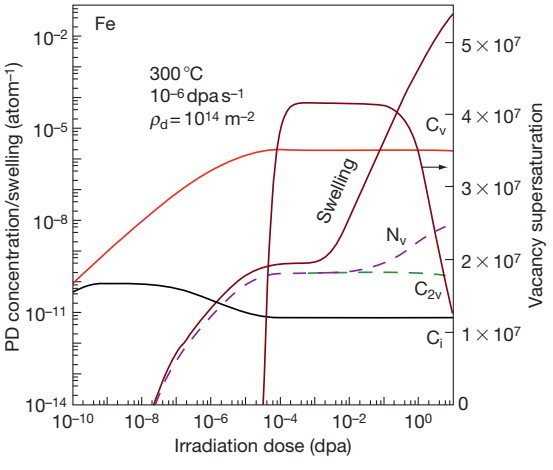

Figure 4 Dose dependences of the concentrations of point defects, void swelling, vacancy supersaturation, and void number density calculated in the framework of FP3DM by numerical integration of the master equation, eqn [18]. From Golubov and Ovcharenko.[73]

If only voids and edge dislocations are present in the system, and mutual recombination and thermal emission of vacancies from voids and dislocations are both negligible, the balance equations for the concentrations of vacancies and SIAs, C_v and C_i, are given by

$$G - k_c^2 D_v C_v - Z_v^d \rho_d D_v C_v = 0$$
$$G - k_c^2 D_i C_i - Z_i^d \rho_d D_i C_i = 0 \quad [93]$$

The defect concentrations, C_v and C_i, are then

$$C_v = \frac{G}{D_v(k_c^2 + Z_v^d \rho_d)}$$
$$C_i = \frac{G}{D_i(k_c^2 + Z_v^d \rho_d)} \quad [94]$$

Hence, taking into account that $Z_v^d \approx Z_i^d$,

$$D_v C_v \approx D_i C_i = \frac{G}{k_c^2 + Z_v^d \rho_d} \quad [95]$$

The swelling rate is equal to the net (excess) flux of vacancies to voids:

$$\frac{\mathrm{d}S}{\mathrm{d}\phi} = k_c^2 [D_v C_v - D_i C_i]$$
$$= B_d \frac{k_c^2 Z_v^d \rho_d}{(k_c^2 + Z_v^d \rho_d)(k_c^2 + Z_i^d \rho_d)} \approx B_d \frac{k_c^2 Z_v^d \rho_d}{(k_c^2 + Z_v^d \rho_d)^2} \quad [96]$$

where $S = (4\pi/3) N_c \langle r_c \rangle^3$ and $\phi = Gt$ are the total volume of voids and the irradiation dose in dpa, respectively; and B_d is the dislocation bias factor

$$B_d = \frac{Z_i^d - Z_v^d}{Z_v^d} \quad [97]$$

The maximum value of the ratio in the right-hand side of eqn [96] is 1/4, when the sink strengths of voids and dislocation are equal to each other, $k_c^2 = Z_v^d \rho_d$. Thus the maximum swelling rate is

$$\left(\frac{\mathrm{d}S}{\mathrm{d}\phi}\right)_{max} = \frac{B_d}{4} \quad [98]$$

It is easy to show that the swelling rate described by eqn [96] depends only weakly on the variation of the sink strength of voids and dislocations: a difference of an order of magnitude results in a decrease of the swelling rate by a factor of 3 only.

To obtain the steady-state swelling rates of ~1% per NRT dpa, which are observed in high-swelling

fcc materials, one would need the bias factor to be about several percent. Data on swelling in electron-irradiated metals resulted in $B_d \approx 2-4\%$ for the fcc copper[24,105,106] (data reported by Glowinski[107] were used in Konobeev and Golubov[106]), ~2% for pure Fe–Cr–Ni alloys,[108] and orders of magnitude lower values for bcc metals (e.g., swelling data for molybdenum[109]). Because the electron irradiation produces FPs, it is reasonable to accept these values as estimates of the dislocation bias.

Note that the first attempt to determine B_d by solving the diffusion equations with a drift term determined by the elasticity theory for PD–dislocation interaction as described in **Section 1.13.5** showed that the bias is significantly larger than the empirical estimate above. Several works have been devoted to such calculations,[96,110–113] which predicted much higher B_d values, for example, ~15% for the bcc iron and ~30% for the fcc copper. With these bias factors, the maximum swelling rates based on $B_d/4$ should be equal to about 4% and 8% per dpa but such values have never been observed. An attempt to resolve this discrepancy can be found in a recent publication.[114]

Surprisingly, the steady-state swelling rate of ~1% per NRT dpa has been found in neutron- (and ion-) irradiated materials, for example, in various stainless steels, even though the primary damage in these cases is known to be very different and the void swelling should be described in the framework of the PBM, which gives a rather different description of the process. An explanation of this is proposed in **Section 1.13.6**.

1.13.5.2.2 Effect of recombination on swelling

Mutual annihilation of PDs happens either by direct interaction between single vacancies and SIAs in the matrix or within a certain type of neutral sink which we call 'saturable.' The fluxes of vacancies and SIAs to them are equal. An example of such sinks is vacancy loops, which were considered in the framework of the BEK model[29] and PBM,[22] that is, in the case where the vacancy clusters are generated in cascades. The BEK model is not discussed further in the present work because it does not correspond to any realistic situation in solids under irradiation; vacancy clustering in cascades is always accompanied with the SIA clustering, which is accounted for in the framework of the PBM but not in the BEK model.

The balance equations in the case considered are as follows

$$\begin{aligned} G - \mu_R D_i C_i C_v - k_N^2 D_i C_i - k_c^2 D_v C_v - Z_v^d \rho_d D_v C_v = 0 \\ G - \mu_R D_i C_i C_v - k_N^2 D_i C_i - k_c^2 D_i C_i - Z_i^d \rho_d D_i C_i = 0 \end{aligned} \quad [99]$$

where k_N^2 is the strength of neutral sinks. Note that absorption rate of both vacancies and SIAs in eqn [99] is described by the same quantity, $k_N^2 D_i C_i$, which reflects neutrality of this sink with respect to vacancies and SIAs.[115,116]

The defect concentrations and swelling rate are

$$D_v C_v \approx D_i C_i = \frac{G}{k_c^2 + Z_v^d \rho_d} \frac{1}{1+f_R} \frac{1}{1+f_N}$$

$$\frac{dS}{d\phi} = B_d \frac{k_c^2 Z_v^d \rho_d}{\left(k_c^2 + Z_v^d \rho_d\right)^2} \frac{1}{1+f_R} \frac{1}{1+f_N} \quad [100]$$

where

$$f_R = \frac{1}{2}\left[\sqrt{1 + \frac{4\mu_R G}{(k_c^2 + Z_v^d \rho_d + k_N^2)^2 D_v}} - 1\right]$$

$$f_N = \frac{k_N^2}{k_c^2 + Z_v^d \rho_d} \quad [101]$$

In the absence of an effect on the sink structure, mutual recombination reactions are important at low temperature, when the vacancy diffusion is slow, and for high defect production rates, when the vacancy concentration is sufficiently high to provide higher sink strength for SIAs than that of existing extended defects. This can be expressed mathematically by an inequality $f_R \geq 1$ or more explicitly as a temperature boundary $k_B T < E_v^m / \ln[2D_{v0}(k_c^2 + Z_v^d \rho_d + k_N^2)^2 / \mu_R G]$ where D_{v0} is the preexponential factor in the vacancy diffusion coefficient and E_v^m is the effective activation energy for the vacancy migration. In practice, this situation is unlikely to occur because the radiation-induced sink strength rapidly increases at low temperatures. In this case recombination at sinks is of greater importance.

One of the important aspects that recombination reactions introduce to microstructural evolution is the appearance of a temperature dependence; at low temperatures, an increase of the swelling rate with increasing temperature is predicted, which is also observed experimentally in the fcc-type materials. The question of whether it was possible to explain the experimental reduction of swelling rate with decreasing temperature by recombination was addressed.[29] It was found that the observed temperature effect on swelling rate was much stronger than predicted by recombination alone.

The impact of neutral sinks on swelling rate is significant when they represent the dominant sink

in the system: $k_N^2 \gg k_c^2 + Z_v^d \rho_d$. The swelling rate in the case is given by

$$\frac{dS}{d\phi} = B_d \frac{k_c^2 Z_v^d \rho_d}{(k_c^2 + Z_v^d \rho_d)(k_c^2 + Z_v^d \rho_d + k_N^2)} \approx B_d \frac{k_c^2 Z_v^d \rho_d}{(k_c^2 + Z_v^d \rho_d) k_N^2} \quad [102]$$

Such a situation may occur, for example, at low enough temperature, when the thermal stability of vacancy loops and SFTs becomes high enough, leading to their accumulation up to extremely high concentrations. Another possibility is when a high density (about $10^{24}\,m^{-3}$) of second phase particles exists, as in the oxide dispersion strengthened (ODS) steels.

1.13.5.2.3 Effect of immobilization of vacancies by impurities

The diffusion coefficient of vacancies is an important parameter for microstructural evolution, for it determines the rate of mutual recombination of PDs. Migrating vacancies can also meet solute or impurity atoms and form immobile complexes, which can then dissociate. In quasi-equilibrium, when the rates of complex formation and dissociation events are equal to each other:

$$z\nu^+ C_v' C_s' = \nu^- C_{vs} \quad [103]$$

Here, C_{vs} and C_s are the concentrations of complexes and solute atoms, respectively, C_s' and C_v' are the concentrations of free (unpaired) solute atoms and vacancies, respectively, ν^+ and ν^- are the frequencies of complex formation and dissociation events, respectively, and z is a geometrical factor, which is of the order of the coordination number for complexes with a short-range (first-nearest neighbor) interaction and unity for long-range interactions. The binding energy of the complex, E_{vs}^b, is defined from $\nu^-/\nu^+ = \exp(\beta E_{vs}^b)$. The solute concentration is generally much higher than that of vacancies, hence

$$C_s' \approx C_s$$
$$C_v' = C_v - C_{vs} \quad [104]$$

Substituting these into eqn [103], one obtains

$$C_{vs} = \frac{\alpha C_v C_s \exp(\beta E_{vs}^b)}{1 + \alpha C_s \exp(\beta E_{vs}^b)} \quad [105]$$

The total vacancy concentration is, therefore,

$$C_v = C_v' + C_{vs} = C_v'\left[1 + \alpha C_s \exp\left(\beta E_{vs}^b\right)\right] \quad [106]$$

The effective diffusion coefficient of vacancies may be defined as

$$D_v^{eff} = \frac{D_v}{1 + \alpha C_s \exp(\beta E_{vs}^b)} \approx \frac{D_{v0}}{\alpha C_s} \exp\left[-\beta(E_v^m + E_{vs}^b)\right] \quad [107]$$

While the vacancy concentration is approximately equal to

$$C_v \approx C_v' \alpha C_s \exp\left(\beta E_{vs}^b\right) \quad [108]$$

The vacancy flux is, thus, equal to that in the absence of impurities,

$$D_v^{eff} C_v = D_v C_v' \quad [109]$$

which is supported by the measurements of the self-diffusion energy, which is almost independent of the presence of impurities. The main conclusion is that the total vacancy flux does not depend on the presence of impurity atoms. However, impurity trapping may affect the recombination rate and hence C_v may be increased.

1.13.5.3 Inherent Problems of the Frenkel Pair, 3-D Diffusion Model

Many observations contradict the FP3DM. These include the void lattice formation[11–14] and higher swelling rates near GBs than in the grain interior in the following cases: high-purity copper and aluminum irradiated with fission neutrons or 600 MeV protons (see original references in reviews[117,118]); aluminum irradiated with 225 MeV electrons[119] and neutron-irradiated nickel[120] and stainless steel.[121] Furthermore, the swelling rate at very low dislocation density in copper is higher,[122–124] and the dependence of the swelling rate on the densities of voids and dislocations is different,[125] than predicted by the FP3DM. It gradually became clear that something important was missing in the theory. There was evidence that this missing part could not be the effect of solute and impurity atoms or the crystal structure. Indeed, austenitic steels of significantly different compositions and swelling incubation periods exhibit similar steady-state swelling rates of ~1% per NRT dpa.[32,33] And, although generally the bcc materials show remarkable resistance to swelling,[31,33] the alloy V–5% Fe showed the highest swelling rate of ~2% per dpa: 90% at 30 dpa.[34]

As outlined in **Section 1.13.3.1**, the primary damage production under neutron and ion irradiations is more complicated; in addition to PDs, both vacancy

and SIA clusters are produced in the displacement cascades. This is the reason the FP3DM predictions fail to explain microstructure evolution in solids under cascade damage conditions. In fact, it has been shown that it is the clustering of SIAs rather than vacancies that dominates the damage accumulation behavior under such conditions. The PBM proposed in the early 1990s and developed during the next 10 years (see **Section 1.13.1**) essentially resolved many of the issues; the phenomena mentioned have been properly understood and described. This model is described in the next section.

1.13.6 Production Bias Model

The continuous production of SIA clusters in displacement cascades is a key process, which makes microstructure evolution under cascade conditions qualitatively different from that during FP producing 1 MeV electron irradiation. In this case, eqns [10]–[12] should be used for the concentration of mobile defects. The equations for isolated PDs have been considered in detail in the previous section. In order to analyze damage accumulation under cascade irradiation, one needs to define the sink strengths of various defects for the SIA mobile clusters in eqn [12]. We give examples of such calculations for the case when cluster migrates 1D rather than 3D in the following section.

1.13.6.1 Reaction Kinetics of One-Dimensionally Migrating Defects

The 1D migration of the SIA clusters along their Burgers vector direction results in features that distinguish their reaction kinetics from 3D diffusing defects. These were first noticed in and theoretically analyzed for annealing experiments (Lomer and Cottrell,[126] Frank *et al.*,[127] Gösele and Frank,[128] Gösele and Seeger,[129] and Gösele[40]) and, then, under irradiation (Trinkaus *et al.*[19,20] and Borodin[130]). In this section, we consider the reaction kinetics of 1D migrating clusters with immobile sinks and follow the procedure employed in Barashev *et al.*[25]

Detailed information about the diffusion process of a 1D migrating particle is given by the function $u(t,\xi,x)$, which is known as Furth's formula for first passages and has the following probabilistic significance.[131] In a diffusion process starting at the point $\xi > 0$, the probability that the particle reaches the origin before reaching the point $x > \xi$ in the time interval $t_1 < t < t_2$ is given by the integral over this interval. For particles undergoing random walk, this function is found to be equal to

$$u(t,\xi,x) = 2\pi \sum_{i=1}^{\infty} i \exp\left[\frac{-i^2\pi^2 D_{1D} t}{x^2}\right] \sin\left(\frac{i\pi\xi}{x}\right) \quad [110]$$

where D_{1D} is the diffusion coefficient. Using this function, one can write the probability for a particle to survive until time t, that is, not to be absorbed by the barriers placed at the origin and at the point x, as

$$\eta(t,\xi,x) = \int_t^{\infty} dt' \left[u(t',\xi,x) + u(t',x-\xi,x)\right]$$
$$= \frac{4}{\pi} \sum_{i=1}^{\infty} \frac{\exp\left[-(2i-1)^2\pi^2 D_{1D} t/x^2\right]}{2i-1} \sin\left(\frac{\pi\xi(2i-1)}{x}\right) \quad [111]$$

The expected duration of the particle motion until its absorption is given by:

$$\tau_{ruin}(\xi,x) = \int_0^{\infty} \eta(t,\xi,x)dt = \frac{\xi(x-\xi)}{2D_{1D}} \quad [112]$$

Equation [112] is the classical result of the 'gambler's ruin' problem considered by Feller.[131]

1.13.6.1.1 Lifetime of a cluster

In order to obtain the lifetime of 1D migrating clusters, one should average $\tau_{ruin}(\xi,x)$ over all possible distances between sinks and initial positions of the clusters, that is, over x and ξ. For this purpose, the corresponding probability density distribution, $\varphi(x,\xi)$, is required.

Let us assume that all sinks are distributed randomly throughout the volume and introduce the 1D density of traps (sinks), Λ, that is, the number of traps per unit length. In this case, $\varphi(x,\xi)$ can be represented as a product of the probability density for a cluster to find itself between two sinks separated by a distance x, $\Lambda^2 x \exp(-\Lambda x)$, and the probability density to find a cluster at a distance ξ from one of these sinks, $1/x$:

$$\varphi(x,\xi) = \Lambda^2 \exp(-\Lambda x), 0 < x < \infty, 0 < \xi < x \quad [113]$$

With this distribution, the cluster lifetime, τ_{1D}, and the mean-free path to sinks, λ, are:

$$\tau_{1D} = \langle \tau_{ruin}(\xi,x) \rangle_{\xi,x} = 1/2D_{1D}\Lambda^2 \quad [114]$$

$$\lambda = \langle \xi \rangle_{\xi,x} = 1/\Lambda \quad [115]$$

where the brackets denote averaging: $\langle\rangle_{\xi,x} = \int_0^{\infty} dx \int_0^{x} d\xi \varphi(x,\xi)$

1.13.6.1.2 Reaction rate

It follows from eqn [114] that the reaction rate between 1D migrating clusters and immobile sinks (e.g., Borodin[130]) is given by:

$$R_{1D} = 2\Lambda^2 D_{1D} C = \frac{2}{\lambda^2} D_{1D} C \qquad [116]$$

This equation defines the total reaction rate as a function of Λ, determined by the concentration and geometry of sinks. If there are different sinks in the system, Λ is a sum of corresponding contributions Λ_j from traps of type j. In a crystal containing dislocations and voids only,

$$\Lambda = \Lambda_d + \Lambda_c \qquad [117]$$

where subscripts 'd' and 'c' stand for dislocations and voids, respectively. These partial trap densities are found below.

Consider voids of a particular radius r_i randomly distributed over the volume. Without loss of generality, the capture radius of a void for a cluster is assumed here to be equal to its geometrical radius, that is, $r_{ci} = r_i$. A void of radius r_i is available to react with mobile clusters that lie in a cylinder of this radius around the cluster path. Hence, the partial 1D density of voids of any particular radius, Λ_{ci}, and the total 1D void density, Λ_c, are given by

$$\Lambda_{ci} = \pi r_{ci}^2 f(r_i) \qquad [118]$$

$$\Lambda_c = \sum_i \Lambda_{ci} = \pi r_c^2 N_c \qquad [119]$$

where $f(r_i)$ is the SDF of voids ($\sum_i f(r_i) = N_c$ is the total void number density) and r_c^2 is the mean square of the void capture radius. For dislocations

$$\Lambda_d = \pi r_d \rho_d^* \qquad [120]$$

where ρ_d^* is the dislocation density defined as the mean number of dislocation lines intersecting a unit area (surface density) and r_d is the corresponding capture radius. This can be shown in the following way. The mean number of dislocation lines intersecting the cylinder of unit length and radius r_d around the cluster path equals the area of the cylinder surface, $2\pi r_d$, times the dislocation density divided by 2. (The factor 2 arises because each dislocation intersects the cylinder twice.) It should be noted that the dislocation sink strength for 3D diffusing defects is usually expressed through the dislocation density, ρ_d, defined as the total length of dislocation lines per unit volume of crystal (volume density). The relationship between ρ_d^* and ρ_d depends on the distribution of the dislocation line directions. For a completely random arrangement, the volume density is twice the surface density, $\rho_d \approx 2\rho_d^*$ (see, e.g., Nabarro[132]). In this case, eqn [120] is the same as found by Trinkaus *et al.*[19,20]

Substituting eqns [117]–[120] into eqn [116], the total reaction rate of the clusters in a crystal containing random distribution of voids and dislocations is found to be[130]:

$$R_{1D} = 2\left(\frac{\pi r_d \rho_d}{2} + \pi r_c^2 N_c\right)^2 D_{1D} C \qquad [121]$$

For the case, in which immobile vacancy and SIA clusters are also taken into account, the sink strength for 1D diffusing SIA clusters, k_g^2, is equal to

$$k_g^2 = 2\left(\frac{\pi r_d \rho_d}{2} + \pi r_c^2 N_c + \sigma_{vcl} N_{vcl} + \sigma_{icl} N_{icl}\right)^2 \qquad [122]$$

where σ_{vcl} and σ_{icl} are the interaction cross-sections and N_{vcl} and N_{icl} the number densities of the sessile vacancy and SIA clusters, respectively. σ_{vcl} and σ_{icl} are proportional to the product of the loop circumference and the corresponding capture radius similar to r_d for dislocations.

1.13.6.1.3 Partial reaction rates

A detailed description of the microstructure evolution requires the partial reaction rates, R_j, of the clusters with each particular sink, for example, dislocations or voids of various sizes.[22] According to the definition of the parameters Λ_j and Λ, the ratio Λ_j/Λ is the probability for a trap to be of type j. Hence, the partial reaction rates are

$$R_j = \left(\frac{\Lambda_j}{\Lambda}\right) R \qquad [123]$$

A similar relation between total and partial reaction rates was used in Gösele and Frank.[128] Using eqn [116], one can write the partial reaction rate of clusters with sinks of type j

$$R_j = 2\Lambda_j \Lambda D_{1D} C = \frac{2}{\lambda \lambda_j} D_{1D} C \qquad [124]$$

where $\lambda_j = 1/\Lambda_j$ is the mean distance between a cluster and a sink of type j in 1D, cf. eqn [116]. Thus, the partial reaction rate of a specific type of sink depends on the density of that sink and also on the density of all other sinks. This correlation between sinks is characteristic of pure 1D diffusion–reaction kinetics in contrast to 3D diffusion where the leading term of the sink strength of any defect is not correlated with others (see eqn [54]).

1.13.6.1.4 Reaction rate for SIAs changing their Burgers vector

It has been suggested that deviations of the SIA cluster diffusion from pure 1D mode may significantly alter their interaction rate with stable sinks.[23] These deviations could have different reasons, such as thermally activated changes of the Burgers vector of glissile SIA clusters, as observed in MD simulation studies for clusters of two and three SIAs. The reaction rate in the case has been calculated previously[25,27]; here we present the main result only.

If τ_{ch} is the mean time delay before Burgers vector change and $l = \sqrt{2D_{1D}\tau_{ch}}$ is the corresponding MFP, then the reaction rate can be approximated by the following function[25]:

$$R \approx \frac{l^2}{2\lambda^2}\left[1 + \left(1 + \frac{8\lambda^2}{l^2}\right)^{1/2}\right]\frac{C}{\tau_{ch}} \qquad [125]$$

which gives the correct value in the limiting case of pure 1D diffusion, when $\tau_{ch} \to \infty$, and a correct description of increasing reaction rate with decreasing τ_{ch}. The analysis is valid for values of l larger than the mean void and dislocation capture radii, and overestimates reaction rates in the limiting case of 3D diffusion, see paragraph 6 in Barashev *et al.*[25] for details. Similar functional form of the reaction rate is obtained by employing an embedding procedure,[27] which gives a correct description over the entire range of l in the case when voids are the dominant sinks in the system.

1.13.6.1.5 The rate P(x) for 1D diffusing self-interstitial atom clusters

In the case where 1D migrating SIA clusters are generated during irradiation in addition to PDs, the ME has to account for their interaction with the immobile defects. In the simplest case where the mean-size approximation is used for the clusters, $G^{g}_{icl}(x) = G^{g}\delta(x - x_g)$, the ME for the defects such as voids or vacancy and SIA loops takes a form[22]

$$\begin{aligned}\partial f^{s}(x,t)/\partial t = {} & G^{s}(x) + \mathcal{J}(x-1,t) \\ & - \mathcal{J}(x,t) - P_{1D}(x) f^{s}(x) \\ & \pm P_{1D}(x \mp x_g) f^{s}(x \mp x_g),\ x \geq 2\end{aligned} \qquad [126]$$

where $P_{1D}(x)$ is the rate of glissile loop absorption by the defects. The $\pm$ and $\mp$ in eqn [126] are used to distinguish between vacancy-type defects (voids and vacancy loops/SFT) and SIA type because capture of SIA glissile clusters leads to a decrease in the size in the former case and an increase in the latter one.

The rate $P_{1D}(x)$ depends on the type of immobile defects. In the case of voids, their interaction with the SIA clusters is weak and therefore the cross-sections may be approximated by the corresponding geometrical factor equal to $\pi R_v^2 N_v$. The rate $P_{1D}(x)$ in this case is given by (see eqn [11c] in Singh *et al.*[22])

$$P_{1D}(x) = 2\left(\frac{3\sqrt{\pi}}{4}\right)^{2/3}\frac{\Lambda D_g C_g}{\Omega^{1/3}}x^{2/3} \qquad [127]$$

where $\Lambda = \sqrt{k_g^2/2}$. Note that the factor 2 in eqn [127] was missing in Singh *et al.*[22]

In the case of dislocation loops, the situation is more complicated as the cross-section is defined by long-range elastic interaction. A fully quantitative evaluation is rather difficult because of the complicated spatial dependence of elastic interactions, in particular, for elastically anisotropic media. For loops of small size, the effective trapping radii turn out to be large compared with the geometrical radii of the loops and hence the 'infinitesimal loop approximation' may be applied. It is shown (see Trinkaus *et al.*[20]) that in this case the cross-section is proportional to $(xx_g)^{1/3}$ thus the rate $P_{1D}(x)$ is equal to

$$P_{1D}(x) = \frac{2.25\pi\eta}{\Omega^{1/3}}\left(\frac{x_g T_m}{T}\right)^{2/3}\Lambda D_g C_g x^{2/3} \qquad [128]$$

where T and T_m are temperature and melting temperature, the multiplier η is a correction factor which is introduced because eqn [4] in Trinkaus *et al.*[20] was obtained using some approximations of the elastically isotropic effective medium and, consequently, it can be considered as a qualitative estimate of the cross-section rather than a quantitative description. The factor η is of order unity and was introduced as a fitting parameter. Since sessile SIA and vacancy clusters have different structures (loops in the case of the SIA clusters and frequently SFTs in the case of vacancy clusters), the multiplier η and, consequently, the appropriate cross-sections may be slightly different. Also note that $\mu\Omega = k_B T_m$ has been used in Trinkaus *et al.*[20] as an estimate on a homologous basis.

In the case of large size dislocation loops, the cross-section of their interaction with the SIA glissile clusters can be calculated in a way similar to that of edge dislocations. Namely, it is proportional to the product of the length of dislocation line, that is, $2\pi R_l$, and the capture radius, b_l. The rate $P_{1D}(x)$ in that case is given by

$$P_{1D}(x) = 4\sqrt{\frac{\pi}{\Omega b}}b_l \Lambda D_g C_g x^{1/2} \qquad [129]$$

Note that in the more general case where different sizes of the SIA glissile clusters are taken into account, the last term on the right side of eqn [126] has to be replaced with the sum $\sum_{y=x_g^{min}}^{y=x_g^{max}} P_{1D}(x \mp y) f(x \mp y)$.

1.13.6.1.6 Swelling rate

By omitting the recombination term, eqns [10]–[12] for mobile defects can be rewritten as

$$\frac{dC_v}{dt} = G_v + G_{vc} - D_v C_v (k_c^2 + Z_v^d \rho_d + Z_v^{icl} k_{icl}^2 + Z_v^{vcl} k_{vcl}^2)$$
$$\frac{dC_i}{dt} = G_i - D_i C_i (k_c^2 + Z_i^{vcl} \rho_d + Z_i^{icl} k_{icl}^2 + Z_i^{vcl} k_{vcl}^2)$$
$$\frac{dC_{icl}^g}{dt} = G_i^g - 2D_g C_g \left(\frac{\pi r_d \rho_d}{2} + \pi r_c^2 N_c + \sigma_{vc} N_{vcl} + \sigma_{ic} N_{icl}\right)^2 \quad [130]$$

It has been shown that, under conditions in which swelling is observed, the vacancy and SIA clusters produced by cascades reach steady-state size distributions at relatively small doses.[22] This is because vacancy clusters have far lower thermal stability than voids. The growth of sessile SIA clusters is restricted on account of the high vacancy supersaturation, which builds up due to rapid 1D diffusion of mobile SIA clusters to sinks. Consequently, at relatively low doses, the SDF of the sessile SIA clusters achieves steady state. After reaching steady state, both types of sessile clusters start to serve as recombination centers for PDs and glissile SIA clusters. Analytical expressions for the steady-state SDFs of vacancy and SIA clusters can be found (see eqns [23] and [24] in Singh *et al.*[22]) and the corresponding sink strengths of the clusters at the steady state are given by (eqn [25] in the same reference)

$$k_{vcl}^2 = \frac{\epsilon_v^s G_v}{D_v \exp(-E_{vcl}/k_B T)(k_c^2 + Z_v^d \rho_d) - \epsilon_i^g G_v} (k_c^2 + Z_v^d \rho_d)\left(1 - \frac{1}{x_{vcl}^s}\right) \quad [131]$$

$$k_{icl}^2 = \frac{\epsilon_i^s}{\epsilon_i^g}(k_c^2 + Z_i^d \rho_d)\left(1 - \frac{1}{x_{icl}^s}\right) \quad [132]$$

where E_{vcl} is an effective binding energy of vacancies with the vacancy clusters and $x_{vcl,icl}^s$ are the mean size of the vacancy and SIA glissile clusters (see eqn [8]).

It should be noted that the SDF of sessile interstitial clusters, the sink strength of which is described by eqn [132], is limited by the maximum size of the clusters produced in displacement cascades (see **Figure 2** in Singh *et al.*[22]). This is because the clusters produced are reduced in size due to the high vacancy supersaturation. Fluctuations in the defect arrival to the clusters produce a tail in the SDF extending beyond the maximum size formed in cascades. The tail is characterized by very small concentrations and cannot describe the observed nucleation and growth of SIA clusters and the consequent formation of the dislocation network (see, e.g., Garner[32] and Garner *et al.*[33]). The most probable reason for this failure is that the cluster–cluster interaction leading to their coalescence is neglected in the current theoretical framework.

Sessile interstitial clusters are produced in cascades at rates comparable to those of PDs. The evolution of concentrations of mobile species (PDs and glissile clusters) in this case may be described by nonstationary equations because of the very fast evolution of the sessile cluster population. High vacancy supersaturation will drive the evolution of the sessile SIA clusters toward quasisaturation state, beyond which the steady-state equations for the mobile species become valid. Similar steady state for vacancy clusters will be achieved because of the thermal instability of the clusters.[22]

$$G_v = D_v C_v (k_c^2 + Z_v^d \rho_d) + D_v C_v Z_v^{icl} k_{icl}^2 + D_i C_i Z_v^{vcl} k_{vcl}^2 + D_g C_g \Lambda x_g \sigma_{icl} N_{icl} \quad [133]$$

$$G_i = D_i C_i (k_c^2 + Z_i^d \rho_d) + D_v C_v Z_v^{icl} k_{icl}^2 + D_i C_i Z_v^{vcl} k_{vcl}^2 - 2D_g C_g \Lambda x_g \sigma_{icl} N_{icl} \quad [134]$$

$$G_i^g = 2D_g C_g \left(\frac{\pi r_d \rho_d}{2} + \pi r_c^2 N_c + \sigma_{vc} N_{vcl} + \sigma_{ic} N_{icl}\right)^2 \quad [135]$$

In the framework of PBM, the balance equations for PDs depend on the concentration of glissile clusters and, thus, are very different from those in the FP3DM.

The vacancy supersaturation is obtained from the difference between $D_v C_v$ and $D_i C_i$ as given by eqns [133] and [134]

$$D_v C_v - D_i C_i = B_d \frac{Z_v^d \rho_d}{k_c^2 + Z_i^d \rho_d} D_v C_v + \frac{\varepsilon_i^g G^{NRT}(1 - \varepsilon_r)}{k_c^2 + Z_v^d \rho_d}\left(1 - \frac{\sigma_{vcl} N_{vcl} + \sigma_{icl} N_{icl}}{\Lambda_g}\right) \quad [136]$$

where $\Lambda_g = \sqrt{k_g^2/2} = \pi r_d \rho_d/2 + \pi r_c^2 N_c + \sigma_{vcl} N_{vcl} + \sigma_{icl} N_{icl}$. The first and the second terms on the right-hand side of eqn [136] correspond to the actions

of the dislocation bias and the production bias, respectively. As can be seen, the first term depends on the vacancy concentration, and hence on the total sink strength of all defects including PD clusters. The second term also depends on the sink strength of all defects but differently, and describes the distribution of excess of vacancies between voids and dislocations, and their recombination at PD clusters.

In the PBM, the swelling rate is given by

$$\frac{dS}{dt} = k_c^2(D_v C_v - D_i C_i) - 2D_g C_g x_g \Lambda_g \pi r_c^2 N_c \qquad [137]$$

and, with the aid of eqn [136], can be represented as follows

$$\frac{dS}{d\phi} = (1-\varepsilon_r)\left\{ B_d \frac{k_c^2 Z_v^d \rho_d}{(k_c^2 + Z_v^d\rho)(k_c^2 + Z_v^d\rho_d + Z_v^{icl}k_{icl}^2 + Z_v^{vcl}k_{vcl}^2)} + \varepsilon_i^g \left[\frac{k_c^2}{k_c^2 + Z_v^d\rho_d}\left(1 - \frac{\sigma_{vcl}N_{vcl} + \sigma_{icl}N_{icl}}{\Lambda_g}\right) - \frac{\pi r_c^2 N_c}{\Lambda_g}\right]\right\} \qquad [138]$$

where $\phi = G^{NRT}t$ is the NRT irradiation dose. The first term in the brackets on the right-hand side of eqn [138] corresponds to the influence of the dislocation bias and the second one to the production bias. The factor $(1-\varepsilon_r)$ describes intracascade recombination of defects, which is a function of the recoil energy and may reduce the rate of defect production by up to an order of magnitude that can be compared to the NRT value: $(1-\varepsilon_r) \to 0.1$ at high PKA energy (see Section 1.13.3). As indicated by this equation, the swelling rate is a complicated function of dislocation density, dislocation bias factor, and the densities and sizes of voids and PD clusters. It also demonstrates the dependence of the swelling rate on the recoil energy, determined by ε_i^g, which increases with increasing PKA energy up to about 10–20 keV. The main predictions of the PBM are discussed below.

1.13.6.2 Main Predictions of Production Bias Model

As can be seen from eqn [138], the action and consequences of the two biases, the dislocation and production ones, is quite different. As shown in Section 1.13.5, the dislocation bias depends only slightly on the microstructure and predicts indefinite void growth. In contrast, the production bias can be positive or negative, depending on the microstructure. The reason for this is in negative terms in eqn [138]. The first term decreases the action of the production bias due to recombination of the SIA clusters at sessile vacancy and SIA clusters, while the second one arises from the capture of SIA clusters by voids. The latter term may become equal to zero or even negative, hence the combination of the two bias factors does not necessarily lead to a higher swelling rate, as shown in Barashev and Golubov.[35]

1.13.6.2.1 High swelling rate at low dislocation density

As shown in Section 1.13.5, in the framework of FP3DM, the swelling rate depends on the dislocation density and becomes small for a low dislocation density, $dS/d\phi \approx B_d\rho_d/k_c^2 \to 0$ at $\rho_d \to 0$ (see eqn [96]). Thus, it was a common belief that the swelling rate in well-annealed metals has to be low at small doses, that is, when the dislocation density increase can be neglected. Under neutron irradiation, the effect of dislocation bias on swelling is even smaller because of intracascade recombination: $(dS/d\phi)^{FPP3D}_{neutr} = (dS/d\phi)^{FPP3D}_{electr}(1-\varepsilon_r) \ll (dS/d\phi)^{FPP3D}_{electr}$. It has been found experimentally, however, that the void swelling rate in fully annealed pure copper irradiated with fission neutrons up to about 10^{-2} dpa (see Singh and Foreman[18]) is of ~1% per dpa, which is similar to the maximum swelling rate found in materials at high enough irradiation doses. This observation was one of those that prompted the development of the PBM. The production bias term in eqn [138] allows the understanding of these observations. Indeed, at low doses of irradiation, the void size is small, and therefore, the void cross-section for the interaction with the SIA glissile clusters is small $(\pi r_c^2 N_c/\Lambda_g \ll 1)$. As a result, the last term in the production bias term is negligible and thus the swelling rate is driven by the production bias:

$$\left(\frac{dS}{d\phi}\right)_{max} \approx (1-\varepsilon_r)\varepsilon_i^g \frac{k_c^2}{k_c^2 + Z_v^d\rho_d} \qquad [139]$$

As in the case $Z_v^d\rho_d \ll k_c^2$, the swelling rate is determined by the cascade parameters $dS/d\phi \approx (1-\varepsilon_r)\varepsilon_i^g k_c^2/(k_c^2 + Z_v^d\rho_d) \approx (1-\varepsilon_r)\varepsilon_i^g$. It has been shown[22,24] that a good agreement with observations is achieved with the following parameters: $1-\varepsilon_r = 0.1$ and $\varepsilon_i^g = 0.2$, which are in good agreement with the results of MD simulations of cascades.

It is worth emphasizing that the value $(1-\varepsilon_r)\varepsilon_i^g$ determines the maximum swelling rate, which can be produced by the production bias. Indeed, assuming that for some reason (see Section 1.13.7) there is no interaction of the mobile SIA clusters with voids and

sessile vacancy and SIA clusters, the swelling rate is given by $dS/d\phi \approx 1/2(1-\varepsilon_r)\varepsilon_i^g$ where the sink strength ratio, $k_c^2/(k_c^2 + Z_v^d\rho_d)$, is taken to be equal to $1/2$, as frequently observed in experiments. Taking into account the magnitude of the cascade parameters ε_r and ε_i^g estimated in Golubov *et al.*[24] and neglecting the dislocation bias term in eqn [138], one may conclude that the maximum swelling rate under fast neutron irradiation may reach about 1% per dpa. As pointed out in **Section 1.13.5**, in the case of FP production, that is, in the FP3DM, the maximum swelling rate is also ~1% per dpa. This coincidence is one of the reasons why an illusion that the FP3DM model is capable of describing damage accumulation in structural and fuel materials in fission and future fusion reactors has survived despite the fact that nearly 20 years have passed since the PBM was introduced.

Note that the production bias provides a way to understand another experimental observation, namely, that the swelling rate in some materials decreases with increasing irradiation dose (see, e.g., **Figure 5** in Golubov *et al.*[24]). Such a decrease is predicted by eqn [138], as the negative term of the production bias, $\pi r_c^2 N_c/\Lambda_g$, increases with an increase in the void size. As the first term in the production bias is proportional to the void radius and the second to the radius squared, the swelling rate may finally achieve saturation at a mean void radius equal to $R_{max} \approx 2\pi r_d$.[19,30,35]

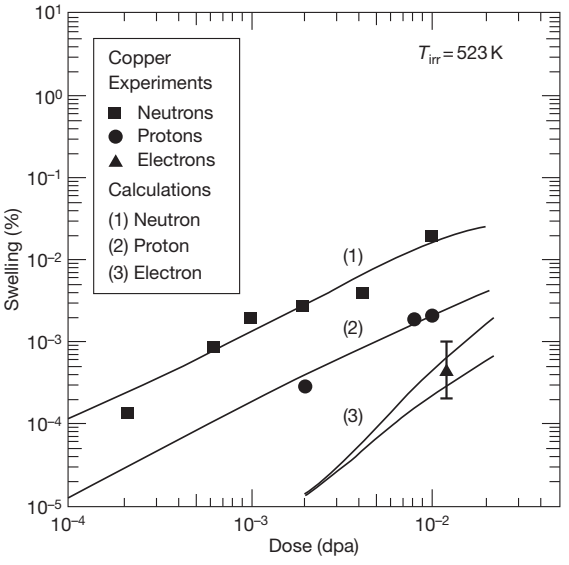

Figure 5 Experimentally measured[133] and calculated[24] levels of void swelling in pure copper after irradiation with 2.5 MeV electrons, 3 MeV protons, and fission neutrons. The calculations were performed in the framework of the FP3DM for the electron irradiation and using the production bias model as formulated in Singh *et al.*[22] for irradiations with protons and fission neutrons. From Golubov *et al.*[24]

Finally, the cascade production of the SIA clusters may strongly affect damage accumulation. As can be seen from eqn [132], the steady-state sink strength of the sessile SIA clusters is inversely proportional to the fraction of SIAs produced in cascades in the form of mobile SIA clusters, thus $k_{icl}^2 \to \infty$ when $\varepsilon_i^g \to 0$. This limiting case was considered by Singh and Foreman[18] to test the validity of the original framework of the PBM,[16,17] where all the SIA clusters produced by cascades were assumed to be immobile (hereafter this case of $\varepsilon_i^g = 0$ is called the *Singh–Foreman catastrophe*). If for some reasons this case is realized, void swelling and the damage accumulation in general would be suppressed for the density of SIA clusters, hence, their sink strength would reach a very high value by a relatively low irradiation dose, $\phi \ll 1$dpa, (see Singh and Foreman[18]). Thus, irradiation with high-energy particles, such as fast neutrons, provides a mechanism for suppressing damage accumulation, which may operate if the SIA clusters are immobilized. In alloys, the interaction with impurity atoms may provide such an immobilization. The so-called 'incubation period' of swelling observed in stainless steels under neutron irradiation for up to several tens of dpa (Garner[32,33]) might be due to the *Singh–Foreman catastrophe*. A possible scenario of this may be as follows: during the incubation period, the material is purified by RIS mainly on SIA clusters because of their high density. At high enough doses, that is, after the incubation period, the material becomes clean enough to provide the recovery of the mobility of small SIA clusters created in cascades that triggered on the production bias mechanism. As a result, the high number density of SIA clusters decreases via the absorption of the excess of vacancies, restoring conditions for damage accumulation.

1.13.6.2.2 Recoil-energy effect

The recoil energy enters the PBM through the cascade parameters ε_r and ε_i^g (see eqn [138]). Direct experimental evaluation of the recoil energy effect on void swelling was made by Singh *et al.*,[133] who compared the microstructure of annealed copper irradiated with 2.5 MeV electrons, 3 MeV protons, and fission neutrons at ~520 K. For all irradiations, the damage rate was $\sim 10^{-8}$ dpa s^{-1}. The average recoil energies in those irradiations were estimated[133]

to be about 0.05, 1, and 60 keV for electron, proton, and neutron irradiations, respectively, thus, producing the primary damage in the form of FPs (electrons), small cascades (protons), and well-developed cascades (neutrons). The cascade efficiency, $1-\varepsilon_r$, hence, the real damage rate, was highest for electron irradiation (no cascades, the efficiency is equal to unity) and minimal for neutron irradiation ($\sim$0.1, see **Section 1.13.3**). If dislocation bias is the mechanism responsible for swelling, the swelling rate is proportional to the damage rate and therefore must be highest after electron and lowest after neutron irradiation. However, just the opposite was found; the swelling level after neutron irradiation was $\sim$50 times higher than after electron irradiation, with the value for proton irradiation falling in between (see **Figure 5**). These results represent direct experimental confirmation that damage accumulation under cascade damage conditions is governed by mechanisms that are entirely different from those under FP production.

The results obtained in this study can be understood as follows. Under electron irradiation, only the first term on the right-hand side of eqn [138] operates, as $\varepsilon_i^g = 0$. The swelling rate is low in this case because of the low dislocation density, as discussed in **Section 1.13.6.2.1**. Under cascade damage conditions, the damage rate is smaller because of the low cascade efficiency. In this case $\varepsilon_i^g \neq 0$ and the second term on the right-hand side of eqn [138] plays the main role, which is evident from the theoretical treatment of the experiment carried out in the following section.[24]

1.13.6.2.3 GB effects and void ordering

As shown in the previous section, several striking observations of the damage accumulation observed in metals under cascade damage conditions can be rationalized in the framework of the PBM. This became possible because of the recognition of the importance of 1D diffusion of SIA clusters, which are continuously produced in cascades. The reaction kinetics in this case are a mixture of those for 1D and 3D migrating defects. Here, we emphasize that 1D transport is the origin of some phenomena, which are not observed in solids under FP irradiation.

One such phenomenon is the enhanced swelling observed near GBs. It is well known that GBs may have significant effect on void swelling. For example, zones denuded of voids are commonly observed adjacent to GBs in electron-, ion-, and neutron-irradiated materials.[134–137] Experimental observations on the effect of grain size on void concentration and swelling in pure austenitic stainless steels irradiated with 1 MeV electrons were also reported.[138,139] In these experiments both void concentration and swelling were found to decrease with decreasing grain size. Theoretical calculations are in good agreement with the grain-size dependence of void concentration and swelling measured experimentally in austenitic stainless steel irradiated with 1 MeV electrons.[139,140]

However, there is a qualitative difference between grain-size dependences of void swelling for electron irradiation and that for higher recoil energies. In particular, in the latter case, in the region adjacent to the void-denuded zone, void swelling is found to be substantially enhanced.[134,136,141–147] Furthermore, in neutron-irradiation experiments on high-purity aluminum, the swelling in the grain interior increases strongly with decreasing grain size.[144] This is opposite to the observations under 1 MeV electron irradiation[139] and to the predictions of a model based on the dislocation bias.[140]

An important feature of the enhanced swelling near GBs under cascade irradiation is its large length scale. The width of this enhanced-swelling zone is of the order of several micrometers, whereas the mean distance between voids is of the order of 100 nm. Thus, the length scale is more than an order of magnitude longer than the mean distance between voids. The MFP of 3D diffusing vacancies and single SIAs is given by

$$L^{3D} = \sqrt{\frac{2}{k^2}} = \sqrt{2}\left(Z^d \rho_d + 4\pi r_c N_c\right)^{-1/2} \qquad [140]$$

and is of the order of the mean distance between defects. Hence, 3D diffusing defects cannot explain the length scale observed. In contrast, the MFP of 1D diffusing SIA clusters is given by

$$L^{1D} = \sqrt{\frac{2}{k_g^2}} = \left(\frac{\pi r_d \rho_d}{2} + \pi r_c^2 N_c\right)^{-1} \qquad [141]$$

and is of the order of several micrometers, hence, exactly as required for explanation of the GB effect (see **Figure 6**). A possible explanation for the observations would be as follows. The SIA clusters produced in the vicinity of a GB, in the region of the size $\sim L^{1D}$, are absorbed by it, while 3D migrating vacancies give rise to swelling rates higher than that in the grain interior. The impact of the GB on the concentration of 1D diffusing SIA clusters can be understood by using local sink strength, that is, the sink strength that depends on the distance of a local

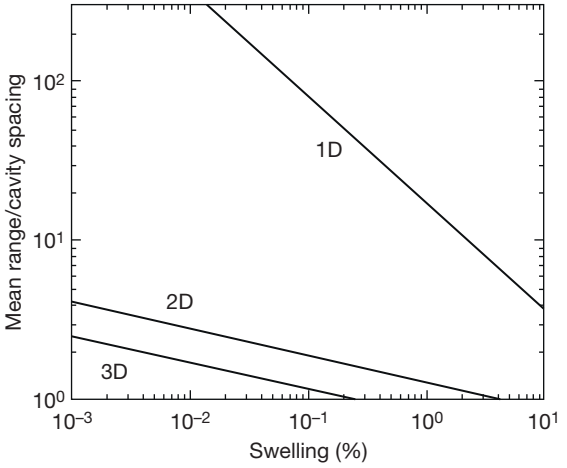

Figure 6 Ratio of the mean-free path of the self-interstitial atom clusters and the distance between voids as a function of void swelling level for 1D, 2D, and 3D migration of the clusters. From Trinkaus, H.; Singh, B. N.; Foreman, A. J. E. *J. Nucl. Mater.* **1993**, *206*, 200–211.

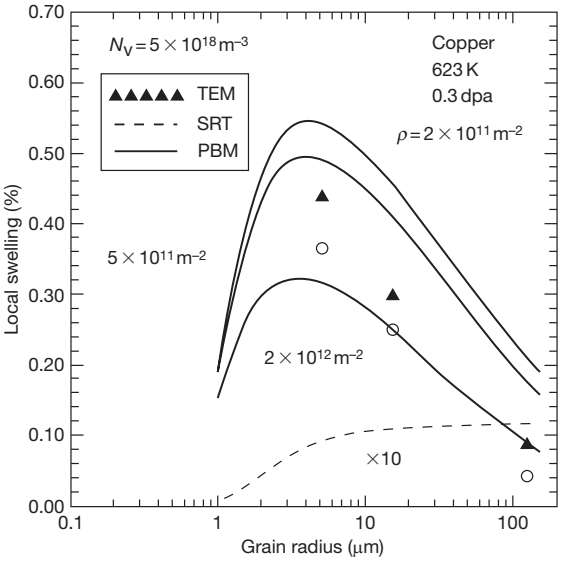

Figure 7 Calculation results on the grain-size dependence of the void swelling in the grain interior in copper irradiated at 623 K to 0.3 dpa. The results are for both the production bias model (PBM) and the FP3DM. The FP3DM values are magnified by a factor of 10. Filled triangles are the measured values. Open circles show calculations using PBM for specific grain sizes and experimental values for void densities and a dislocation density of $12 \times 10^{12}\,m^{-2}$. From Singh, B. N.; Eldrup, M.; Zinkle, S. J.; Golubov, S. I. *Philos. Mag. A* **2002**, *82*, 1137–1158.

area to the GB, l. It has been shown[22] that the local sink strength in a grain of radius R_{GB} is given by

$$k_g^2(R_{GB}, l) = 2\left(\frac{\pi r_d \rho_d}{2} + \pi r_c^2 N_c + \frac{1}{(l(2R_{GB} - l))^{1/2}}\right)^2 \quad [142]$$

As can be seen from eqn [142], the sink strength has a minimum at the center of the grain, that is, at $l = R_{GB}$, and increases to infinity near the GB, when $l \to 0$.

The so-called grain-size effect, an increase of the swelling rate in the grain interior in grains of relatively small sizes (less than about 5 μm) with decreasing grain size, has the same origin as the GB effect discussed above. The swelling rate at the center of a grain may increase with decreasing grain size, when the grain size becomes comparable with the MFP of 1D diffusing SIA clusters and the zones of enhanced swelling of the opposite sides of GBs overlap. The swelling in the center of a grain as a function of grain size is presented in **Figure 7**.[26] For comparison purposes, the values of the local void swelling (see **Table 3** in Singh *et al.*[26]) determined in the grain interiors by TEM are also shown. The PBM predicts a decrease of swelling with increasing grain size for grain radii bigger than 5 μm, which is in accordance with the experimental results. Note that the swelling values calculated by the FP3DM (broken curve in **Figure 7**) are magnified by a factor of 10.

Another striking phenomenon observed in metals under cascade damage conditions is the formation of void lattices. It was first reported in 1971 by Evans[148] in molybdenum under nitrogen ion irradiation, by Kulchinski *et al.*[149] in nickel under selenium ion bombardment, and by Wiffen[150] in molybdenum, niobium, and tantalum under neutron irradiation. Since then it has been observed in bcc tungsten, fcc Al, hcp Mg, and some alloys.[151–155] Jäger and Trinkaus[156] reviewed the characteristics of defect ordering and analyzed the theories proposed at that time, including those based on the elastic interaction between voids and phase instability theory. They concluded that in cubic metals, the void ordering is due to the 1D diffusion of SIA clusters along close-packed crystallographic directions (first proposed by Foreman[157]). Two features of void ordering support this conclusion. First, the symmetry and crystallographic orientation of a void lattice are always the same as those of the host lattice. Second, the void lattices are formed under neutron and heavy-ion but not electron irradiation. This conclusion is also supported by theoretical analysis performed in Hähner and Frank[158] and Barashev and Golubov.[159]

1.13.6.3 Limitations of Production Bias Model

Successful applications of the PBM have been limited to low irradiation doses (<1 dpa) and pure metals (e.g., copper). There are two apparent problems preventing the general application of the model at higher doses.

1.13.6.3.1 Swelling saturation at random void arrangement

The PBM predicts a saturation of void size.[30] This originates from the mixture of 1D and 3D diffusion–reaction kinetics under cascade damage conditions, the assumption lying at the heart of the model. More specifically, it stems from the fact that the interaction cross-section with a void is proportional to the void radius, R, for 3D migrating vacancies and to R^2 for 1D diffusing SIA clusters. As a result, above some critical radius, the latter becomes higher than the former and the net vacancy flux to such voids is negative. In contrast, experiments demonstrate indefinite void growth in the majority of materials and conditions.[31–34] An attempt to resolve this contradiction was undertaken by including thermally activated rotations of the SIA-cluster Burgers vector[23,25,27]; but it has been shown by Barashev *et al.*[25] that this is not a solution. Thus, the PBM fails to account for this important and common observation, that is, the indefinite void growth under cascade irradiation. A way of resolving this issue is discussed in **Section 1.13.7**.

1.13.6.3.2 Absence of void growth in void lattice

Another problem of the PBM is that it fails to explain swelling saturation at rather low swelling levels (approximately several percent) observed in void lattices. In fact, it even predicts an increase in the swelling rate when a random void arrangement is changed to that of a lattice.[25] This is because the free channels between voids along close-packed directions, which are formed during void ordering, provide escape routes for 1D migrating SIA clusters to dislocations and GBs, thereby allowing 3D migrating vacancies to be stored in voids. A possible explanation of the problem is discussed in a forthcoming paper by Golubov *et al.*[37]

1.13.7 Prospects for the Future

As discussed in the previous section, the PBM changed the concept of RDT by recognizing that qualitatively different mechanisms operate in materials when the initial damage is in the form of only FPs and under neutron irradiation, when thermally stable glissile SIA clusters are continuously produced in cascades. The successful applications of the PBM have been limited to low irradiation doses (<1 dpa) and pure metals (e.g., Cu). Furthermore, it predicts the saturation of void size with increasing irradiation dose. Thus, it fails to account for the most important observation under neutron or heavy-ion irradiation: continuous increase in void swelling.

The observed continuous void growth may be explained by the development of *spatial correlations between voids and other lattice defects*. Such as, precipitates and dislocations, that shadow voids from the SIA clusters (see **Figures 8–10**). It has been argued that this must be the case and the very absence of a void lattice (i.e., a particular case of spatial correlation, which is between voids) must be an indication that spatial correlations with other defects prevail.[35]

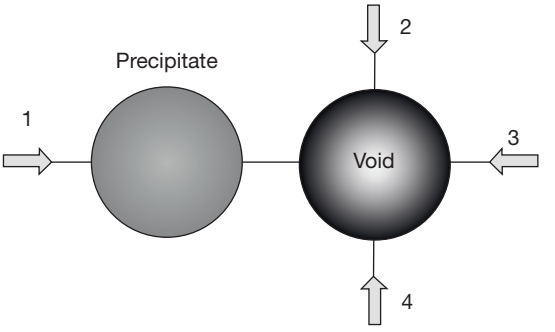

Figure 8 Schematic diagram illustrating screening of a void from self-interstitial atom clusters by a precipitate. The close-packed directions of the cluster Burgers vectors are indicated by arrows. From Barashev, A. V.; Golubov, S. I. *Philos. Mag.* **2009**, *89*, 2833–2860.

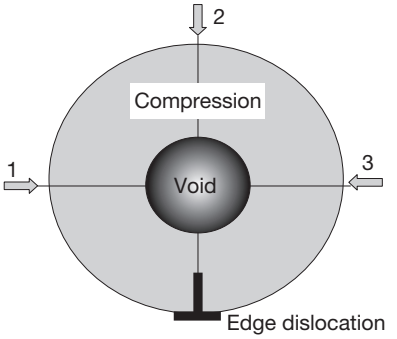

Figure 9 Same as in **Figure 8** but for a void in the compression side of edge dislocation. From Barashev, A. V.; Golubov, S. I. *Philos. Mag.* **2009**, *89*, 2833–2860.

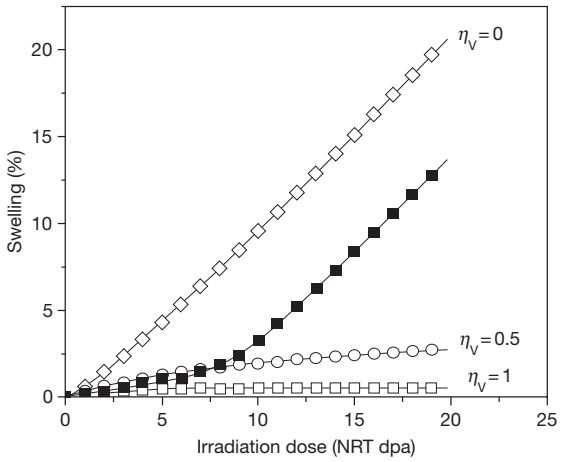

Figure 10 Dependence of swelling on irradiation dose calculated using eqn [143] for $N_c = 10^{22}\text{m}^{-3}$, $r_m = 5$ nm, $\varepsilon_i^g = 0.2$, $\varepsilon_{surv} = 0.1$ and different values of the correlation-screening factor of voids, η_c. The curve with full squares has been calculated for correlations developing with irradiation dose, when $\eta_c = 1$ in the beginning and $\eta_c = 0$ by 10 dpa and higher dose. From Barashev, A. V.; Golubov, S. I. *Philos. Mag.* **2009**, *89*, 2833–2860.

To account for this effect, a new parameter, η_c, has been introduced, called the '*correlation-screening factor*,' which is equal to unity in the absence of shadowing effects and zero when voids are screened completely from the SIA clusters. The swelling rate is then given by

$$\frac{dS}{d\phi} = \varepsilon_i^g \left(1 - \eta_c \frac{r}{r_m}\right) F \qquad [143]$$

where F is a proportionality coefficient, which is a function of all parameters involved.[35] Experimental evidence on the association of large voids with various precipitates (G, η, Laves, etc.)[120,160–162] and the compression side of edge dislocations[163,164] has been available for a long time. More recent evidence can be attributed to Portnykh *et al.*[165] who studied the microstructure of 20% cold-worked 16Cr–15Ni–2Mo–2Mn austenitic steel irradiated up to ~100 dpa in a BN-600 fast reactor in the temperature range from 410 to 600 °C. TEM studies revealed voids of three types: *a-type* associated with dislocations, *b-type* associated with G-phase precipitates and *c-type* distributed homogeneously. The c-type voids were the smallest and made practically no contribution to swelling, while the a-type voids were the largest. Such spatial correlations must be a common feature under cascade irradiation.

As discussed in Barashev and Golubov,[35] the experimental data on void swelling can be fit by eqn [143] with an appropriate choice of the dependence of η_c on the irradiation dose (see **Figure 10**). At high doses, the voids must be completely shielded from the SIA clusters: $\eta_c = 0$, and the steady-state swelling rate of ~1% per dpa observed in austenitic steels[33] can be interpreted as being equal to about half of the production bias, that is, the fraction of SIAs produced as 1D mobile clusters:

$$\frac{dS}{d\phi^{NRT}} \approx \frac{1}{2}\varepsilon_{surv}\varepsilon_i^g \qquad [144]$$

where $\varepsilon_{surv} \equiv (1 - \varepsilon_r) \approx 0.1$ is the survival fraction of defects in displacement cascade. The weak dependence on steel composition observed is probably because the final defect structure is defined by early stages of cascades, when the energies involved are much higher than the binding energies of defects with solute atoms. The observed correlation of the incubation period prior to swelling with the formation of a dislocation network may be connected with an increase of the volume for the nucleation and growth of voids in which voids are screened from the SIA clusters. Higher dislocation density also corresponds to a smaller dislocation climb rate, which might be essential for preserving void-dislocation correlations.

Another distinguishing feature of neutron irradiation is *transmutation of atoms*, which transform even pure metals into alloys with increasing irradiation dose. The atmospheres of solute (or transmuted) elements near voids may repel SIA clusters and, hence, assist or even solely explain the unlimited void growth. It was shown (see, e.g., Golubov,[166] Golubov *et al.*,[167] and references therein) that RIS can provide an additional mechanism of preferential absorption of mobile defects even in the framework of FP3DM, causing a 'segregation' bias, which must be different for immobile defects (e.g., voids) and mobile defects, such as dislocations. In the PBM, the interaction of the mobile SIA clusters with different defects may even be more important. Solute atoms may also decrease the mobility of SIA clusters, thereby increasing the recombination rate with migrating vacancies. In the case of very high binding energy of SIA clusters with impurity atoms, the '*Singh–Foreman catastrophe*'[18] discussed in **Section 1.13.6.2.1** may occur.

Thus, two additional features beyond those already in the PBM distinguish the microstructure evolution under neutron compared to electron irradiation at high enough doses: transmutation of atoms and development of spatial correlations. A fully predictive theory must account for these effects.

The development of a predictive theory requires revisiting all its essential elements: nucleation, growth, movement of voids, and other lattice defects in the presence of spatial correlations, etc. Carefully planned experiments spanning different temperatures, defect production rates, etc., must be a central part of these future studies. Development of the RIS theory for accounting for the SIA clusters is necessary for understanding the sensitivity of microstructure to material composition. Generally, the challenge is to create a theory, where *the mean-field approach in its conventional form is abandoned*, a task not attempted before.

Acknowledgments

The authors would like to acknowledge the fruitful collaboration and discussions on the physics of radiation damage for many years with Professor Yu.V. Konobeev (IPPE, Russia), Drs. B.N. Singh (Risø National Laboratory, Denmark), H. Trinkaus (Forschungscentrum Jülich, Germany), S.J. Zinkle and Yu.N. Osetsky (Oak Ridge National Laboratory, USA), and Professor D.J. Bacon (The University of Liverpool, UK). Various aspects of the author's research discussed in this chapter were supported by the Division of Material Science and Engineering and the Office of Fusion Energy Sciences, Department of Energy and the Office of Nuclear Regulatory Research, US (SIG and RES) and the UK Engineering and Physical Science Research Council (AVB).

References

1. Singh, B. N.; Trinkaus, H.; Golubov, S. I. In *Encyclopedia of Materials: Science and Technology;* Buschow, K. H. J., Cahn, R. W., Flemings, M. C., Ilschner, B., Kramer, E. J., Mahajan, S., Eds.; Oxford: Pergamon, 2001; Vol. 8, pp 7957–7972.
2. Wigner, E. P. *J. Appl. Phys.* **1946**, *17*, 857–863.
3. Seitz, F. *Phys. Today* **1952**, *5*(6), 6–9.
4. Konobeevsky, S. T.; Pravdyuk, N. F.; Kitaitsev, V. I. EFFECT of irradiation on structure and properties of fissionable materials. In *Proceedings of International Conference on Peaceful Uses of Atomic Energy United Nation*, New York; 1955; Vol. 7, pp 433–440.
5. Joseph, J. W., Jr. *Stress Relaxation in Stainless Steel During Irradiation*; USAEC Report DP-369; E.I. Dupont de Nemours and Co., 1955.
6. Cawthorne, C.; Fulton, E. J. *Nature* **1967**, *216*, 575–576.
7. Seeger, A. In *Proceedings of the 2nd UN International Conference of Peaceful Uses of Atomic Energy*, Geneva; United Nation: New York, 1958; Vol. 6, pp 250–273.
8. Kinchin, G. H.; Pease, R. S. *Rep. Prog. Phys.* **1955**, *18*, 1–51.
9. Sizmann, R. *J. Nucl. Mater.* **1968**, *69–70*, 386–412.
10. Mansur, L. K. *J. Nucl. Mater.* **1994**, *216*, 97–123.
11. Evans, J. H. *Nature* **1971**, *229*, 403–404.
12. Evans, J. H. *Radiat. Eff.* **1971**, *10*, 55–60.
13. Kulchinski, G. L.; Brimhall, J. L.; Kissinger, H. I. *J. Nucl. Mater.* **1971**, *40*, 166–174.
14. Wiffen, F. W. In *Proceedings of the 1971 International Conference on Radiation-Induced Voids in Metals (CONF 710601)*; Corbett, J. W., Ianniello, L., Eds.; U.S. Atomic Energy Albany: New York, 1972; pp 386–396.
15. Farrell, K.; Houston, J. T.; Wolfenden, A.; King, R. T.; Jostsons, A. In *Proceedings of the 1971 International Conference on Radiation-Induced Voids in Metals (CONF 710601)*; Corbett, J. W., Ianniello, L., Eds.; U.S. Atomic Energy Albany: New York, 1972; pp 376–385.
16. Woo, C. H.; Singh, B. N. *Phys. Status Solidi B* **1990**, *159*, 609–616.
17. Woo, C. H.; Singh, B. N. *Philos. Mag. A* **1992**, *65*, 889–912.
18. Singh, B. N.; Foreman, A. J. E. *Philos. Mag. A* **1992**, *66*, 975–990.
19. Trinkaus, H.; Singh, B. N.; Foreman, A. J. E. *J. Nucl. Mater.* **1992**, *199*, 1–5.
20. Trinkaus, H.; Singh, B. N.; Foreman, A. J. E. *J. Nucl. Mater.* **1993**, *206*, 200–211.
21. Trinkaus, H.; Singh, B. N.; Woo, C. H. *J. Nucl. Mater.* **1994**, *212–215*, 168–174.
22. Singh, B. N.; Golubov, S. I.; Trinkaus, H.; Serra, A.; Osetsky, Yu. N.; Barashev, A. V. *J. Nucl. Mater.* **1997**, *251*, 107–122.
23. Golubov, S. I.; Singh, B. N.; Trinkaus, H. *J. Nucl. Mater.* **2000**, *276*, 78–89.
24. Golubov, S. I.; Singh, B. N.; Trinkaus, H. O. N. *Philos. Mag. A* **2001**, *81*, 2533–2552.
25. Barashev, A. V.; Golubov, S. I.; Trinkaus, H. *Philos. Mag. A* **2001**, *81*, 2515–2532.
26. Singh, B. N.; Eldrup, M.; Zinkle, S. J.; Golubov, S. I. *Philos. Mag. A* **2002**, *82*, 1137–1158.
27. Trinkaus, H.; Heinisch, H. L.; Barashev, A. V.; Golubov, S. I.; Singh, B. N. *Phys. Rev. B* **2002**, *66*, 060105(R), 1–4.
28. Singh, B. N.; Golubov, S. I.; Trinkaus, H. A general treatment of one- to three-dimensional diffusion reaction kinetics of interstitial clusters: Implications for the evolution of voids; Risø Report No. Risø-R-1644 (EN); 2008.
29. Bullough, R.; Eyre, B. L.; Krishan, K. *Proc. R. Soc. Lond. A* **1975**, *346*, 81–102.
30. Barashev, A. V.; Golubov, S. I. *J. Nucl. Mater.* **2009**, *389*, 407–409.
31. Singh, B. N.; Horsewell, A.; Gelles, D. S.; Garner, F. A. *J. Nucl. Mater.* **1984**, *191–194*, 1172–1176.
32. Garner, F. A. *J. Nucl. Mater.* **1993**, *205*, 98–117.
33. Garner, F. A.; Toloczko, M. B.; Sencer, B. H. *J. Nucl. Mater.* **2000**, *276*, 123–142.
34. Matsui, H.; Gelles, D. S.; Kohno, Y. In *Effects of Radiation on Materials: 15th International Symposium*; Stoller, R. E., Kumar, A. S., Gelles, D. S., Eds.; American Society for Testing and Materials: Philadelphia, PA, 1992; ASTM STP 1125, pp 928–941.
35. Barashev, A. V.; Golubov, S. I. *Philos. Mag.* **2009**, *89*, 2833–2860.
36. Barashev, A. V.; Golubov, S. I. *Mat. Res. Soc. Proc.* **2009**, *1125-R05-04*, 127–132.
37. Golubov, S. I.; Barashev, A. V.; Singh, B. N. On the difference in swelling of bcc and fcc metals under neutron and ion irradiations (in preparation).
38. Laidler, K. J.; King, M. C. *J. Phys. Chem.* **1983**, *87*, 2657–2664.
39. Hänggi, P.; Talkner, P.; Borcovec, M. *Rev. Mod. Phys.* **1990**, *62*, 252–341.

40. Gösele, U. *Prog. React. Kinet.* **1984**, *13*, 63–161.
41. Robinson, M. T. *J. Nucl. Mater.* **1994**, *216*, 1–28.
42. Norgett, M. J.; Robinson, M. T.; Torrens, I. M. *Nucl. Eng. Des.* **1975**, *33*, 50–54.
43. Bacon, D. J.; Osetsky, Yu. N.; Stoller, R. E.; Voskoboinikov, R. E. *J. Nucl. Mater.* **2003**, *323*, 152–162.
44. Calder, A. F.; Bacon, D. J.; Barashev, A. V.; Osetsky, Yu. N. *Philos. Mag.* **2010**, *90*, 863–884.
45. Osetsky, Yu. N.; Bacon, D. J.; Serra, A.; Singh, B. N.; Golubov, S. I. *Philos. Mag.* **2003**, *83*, 61–91.
46. Osetsky, Yu. N.; Bacon, D. J.; Serra, A. *Philos. Mag. Lett.* **1999**, *79*, 273–282.
47. Greenwood, G. W.; Foreman, A. J. E.; Rimmer, D. E. *J. Nucl. Mater.* **1959**, *1*, 305–324.
48. Heald, P. T.; Speight, M. V. *Philos. Mag.* **1974**, *29*, 1075–1080.
49. Wolfer, W. G.; Ashkin, M. *J. Appl. Phys.* **1976**, *47*, 791–800.
50. Bullough, R.; Willis, J. R. *Philos. Mag.* **1975**, *31*, 855–861.
51. Mansur, L. K. *Philos. Mag. A* **1979**, *39*, 497–506.
52. Woo, C. H. *J. Nucl. Mater.* **1984**, *120*, 55–64.
53. Woo, C. H. *J. Nucl. Mater.* **1995**, *225*, 8–14.
54. English, C. A.; Jenkins, M. L. *Philos. Mag.* **2010**, *90*, 821–843.
55. Arakawa, K.; Ono, K.; Isshiki, M.; Mimura, K.; Uchikoshi, M.; Mori, H. *Science* **2007**, *318*, 956–959.
56. Satoh, Y.; Matsui, H. *Philos. Mag.* **2009**, *89*, 1489–1504.
57. Jenkins, M. L.; Yao, Z.; Hernández-Mayoral, M.; Kirk, M. A. *J. Nucl. Mater.* **2009**, *389*, 197–202.
58. Hiroaki, A.; Naoto, S.; Tadayasu, T. *Mater. Trans.* **2005**, *46*, 433–439.
59. Brailsford, A. D.; Bullough, R.; Hayns, M. R. *J. Nucl. Mater.* **1976**, *60*, 246–256.
60. Brailsford, A. D. *J. Nucl. Mater.* **1976**, *60*, 257–278.
61. Brailsford, A. D.; Bullough, R. *Philos. Trans. R. Soc. Lond. A* **1981**, *302*, 87–137.
62. Stoller, R. E.; Golubov, S. I.; Becquart, C. S.; Domain, C. *J. Nucl. Mater.* **2008**, *382*, 77–90.
63. Farkas, L. *Z. Phys. Chem. Leipzig A* **1927**, *125*, 236–242.
64. Becker, R.; Döring, W. *Ann. Phys. Leipzig* **1935**, *24*, 719–752.
65. Zeldovich, J. B. *J. Exp. Theor. Phys.* **1943**, *12*, 525–538.
66. Frenkel, J. *Kinetic Theory of Liquids*; Oxford University Press: New York, 1946.
67. Goodrich, F. G. *Proc. R. Soc. Lond. A* **1964**, *277*, 155–166.
68. Goodrich, F. G. *Proc. R. Soc. Lond. A* **1964**, *277*, 167–182.
69. Feder, J.; Russell, K. C.; Lothe, J.; Pound, G. M. *Adv. Phys.* **1966**, *15*, 111–178.
70. Wagner, R.; Kampmann, R. In *Materials Science and Technology, A Comprehensive Treatment;* Cahn, R. W., Haasen, P., Kramer, E. J., Eds.; VCH: Weinheim, 1991; Vol. 10 B, Part II, pp 213–302.
71. Katz, J. L.; Wiedersich, H. *J. Chem. Phys.* **1971**, *55*, 1414–1434.
72. Russell, K. C. *Acta Metall.* **1971**, *19*, 753–758.
73. Golubov, S. I.; Ovcharenko, A. M. Unpublished.
74. Hayns, M. R. *J. Nucl. Mater.* **1975**, *56*, 267–274.
75. Kiritani, M. *J. Phys. Soc. Jpn.* **1973**, *56*, 95–107.
76. Bondarenko, A. I.; Konobeev, Yu. V. *Phys. Status Solidi A* **1976**, *34*, 195–205.
77. Ghoniem, N. M.; Sharafat, S. *J. Nucl. Mater.* **1980**, *92*, 121–135.
78. Stoller, R. E.; Robert Odette, G. In *13th International Symposium on Radiation Induced Changes in Microstructure*; Garner, F. A., Packan, N. H., Kumar, A. S., Eds.; ASTM: Philadelphia, PA, 1987; ASTM STP 955, Part I, pp 371–392.
79. Hardouin Duparc, A.; Moingeon, C.; Smetniansky-de-Grande, N.; Barbu, A. *J. Nucl. Mater.* **2002**, *302*, 143–155.
80. Wehner, M. F.; Wolfer, W. G. *Phys. Rev. A* **1985**, *52*, 189–205.
81. Ghoniem, N. M. *Phys. Rev. B* **1989**, *39*, 11810–11819.
82. Surh, M. P.; Sturgeon, J. B.; Wolfer, W. G. *J. Nucl. Mater.* **2004**, *325*, 44–52.
83. Clement, C. F.; Wood, M. H. *Proc. R. Soc. Lond. A* **1979**, *368*, 521–546.
84. Koiwa, M. *J. Phys. Soc. Jpn.* **1974**, *37*, 1532.
85. Golubov, S. I.; Ovcharenko, A. M.; Barashev, A. V.; Singh, B. N. *Philos. Mag. A* **2001**, *81*, 643–658.
86. Lifshitz, I. M.; Slezov, V. V. *J. Phys. Chem. Solids* **1961**, *19*, 35–50.
87. Wagner, C. *Z. Elektrochem.* **1961**, *65*, 581–611.
88. Greenwood, G. W.; Speight, M. V. *J. Nucl. Mater.* **1963**, *10*, 140–144.
89. Ovcharenko, A. M.; Golubov, S. I.; Woo, C. H.; Huang, H. *Comput. Phys. Commun.* **2003**, *152*, 208–226.
90. Golubov, S. I.; Stoller, R. E.; Zinkle, S. J.; Ovcharenko, A. M. *J. Nucl. Mater.* **2007**, *361*, 149–159.
91. Surh, M. P.; Sturgeon, J. B.; Wolfer, W. G. *J. Nucl. Mater.* **2004**, *325*, 44; *J. Nucl. Mater.* **2004**, *328*, 107; *J. Nucl. Mater.* **2004**, *336*, 217; *J. Nucl. Mater.* **2005**, *341*, 235–236.
92. Brailsford, A. D.; Bullough, R. *J. Nucl. Mater.* **1972**, *44*, 121–135.
93. Wiedersich, H. *Radiat. Eff.* **1972**, *12*, 11–125.
94. Golubov, S. I.; Minashin, A. M. *Phys. Met. Metall.* **1983**, *56*, 41–46.
95. Ham, F. S. *J. Appl. Phys.* **1959**, *30*, 915–926.
96. Wolfer, W. G. *Comput. Aided Mater. Des.* **2007**, *14*, 403–417.
97. Seeger, A.; Gösele, U. *Phys. Lett. A* **1977**, *61*, 423–425.
98. Singh, B. N.; Eldrup, M.; Zinkle, S. J.; Golubov, S. I. *Philos. Mag. A* **2002**, *82*, 1137–1158.
99. Golubov, S. I. *Phys. Met. Metall.* **1987**, *64*, 40–46.
100. Mikhlin, E. Y.; Nelaev, V. V. *Fizika Metal. i Metalloved.* **1976**, *41*, 1090–1092.
101. Drittler, K.; Lahann, H. J.; Wollenberger, H. *Radiat. Eff. Def. Solids* **1969**, *2*, 51–56.
102. Barashev, A. V.; Golubov, S. I.; Osetsky, Yu. N.; Stoller, R. E. *Philos. Mag.* **2010**, *90*, 907–921.
103. Golubov, S. I. *Phys. Met. Metall.* **1989**, *67*, 32–39.
104. Golubov, S. I. *Phys. Met. Metall.* **1985**, *60*, 7–13.
105. Barlow, P. Ph.D. Thesis, University of Sussex, 1977.
106. Konobeev, Yu. V.; Golubov, S. I. In *Proceedings of 15th International Symposium on Effects of Radiation on Materials*; Stoller, R. E., Kumar, A. S., Gelles, D. S., Eds.; American Society for Testing and Materials: Philadelphia, PA, 1992; ASTM STP 1125, pp 569–582.
107. Glowinski, L. D. *J. Nucl. Mater.* **1976**, *61*, 8–21.
108. Walters, G. P. *J. Nucl. Mater.* **1985**, *136*, 263–279.
109. Igata, N.; Kohyama, A.; Nomura, S. *J. Nucl. Mater.* **1981**, *103–104*, 1157–1162.
110. Heald, P. T. *Philos. Mag.* **1975**, *31*, 551–558.
111. Heald, P. T.; Miller, K. M. *J. Nucl. Mater.* **1976**, *66*, 107–111.
112. White, R. J.; Fisher, S. B.; Heald, P. T. *Philos. Mag.* **1976**, *34*, 647–652.
113. Miller, K. M. *J. Nucl. Mater.* **1979**, *84*, 167–172.
114. Golubov, S. I.; Barashev, A. V.; Singh, B. N.; Stoller, R. E. *Fusion Materials Semiannual Progress Report*; DOE-ER-0313/48; US Department of Energy: Washington, DC, 2010; pp 118–132.

115. Heald, P. T.; Speight, M. V. *J. Nucl. Mater.* **1977**, *64*, 139–144.
116. Golubov, S. I. *Phys. Met. Metall.* **1981**, *52*, 86–94.
117. Singh, B. N.; Zinkle, S. J. *J. Nucl. Mater.* **1993**, *206*, 212–229.
118. Singh, B. N. *Radiat. Eff.* **1999**, *148*, 383–446.
119. Singh, B. N.; Bilde-SØrensen, J. B.; Leffers, T. *J. Nucl. Mater.* **1984**, *122–123*, 542–546.
120. Stiegler, J. O.; Bloom, E. E. *Radiat. Eff.* **1971**, *8*, 33–41.
121. Stoller, R. E.; Odette, G. R. *J. Nucl. Mater.* **1988**, *154*, 286–304.
122. Singh, B. N.; Leffers, T. *Vop. At. Nauki Tekh. Ser. Fiz. Radiat. Povrezh. Radiat. Mater.* **1981**, *15*, 3–18.
123. Singh, B. N.; Leffers, T.; Horsewell, A. *Philos. Mag. A* **1986**, *53*, 233–242.
124. English, C. A.; Eyre, B. L.; Muncie, W. *Philos. Mag. A* **1987**, *56*, 453–484.
125. Cawthorne, C. In *Proceedings of UK/US Fast Reactor Exchange Meeting on Cladding and Duct Materials, CONF-7910113*, HEDL, Richland, Oct 30–Nov 2, 1979; pp 155–161.
126. Lomer, W. M.; Cottrell, A. H. *Philos. Mag.* **1955**, *46*, 711–719.
127. Frank, W.; Seeger, A.; Schottky, G. *Phys. Status Solidi* **1965**, *8*, 345–356.
128. Gösele, U.; Frank, W. *Phys. Status Solidi B* **1974**, *61*, 163–172.
129. Gösele, U.; Seeger, A. *Philos. Mag.* **1976**, *34*, 177–193.
130. Borodin, V. A. *Physica A* **1998**, *260*, 467–478.
131. Feller, W. *An Introduction to Probability Theory and Its Applications*; Willey: New York, 1950; Vol. 1.
132. Nabarro, F. R. N. *Theory of Crystal Dislocations, The International Series of Monographs on Physics*; Oxford University Press: Oxford, 1967.
133. Singh, B. N.; Eldrup, M.; Horsewell, A.; Earhart, P.; Dworschak, F. *Philos. Mag.* **2000**, *80*, 2629–2650.
134. Hudson, J. A.; Mazey, D. J.; Nelson, R. S. *J. Nucl. Mater.* **1971**, *41*, 241–256.
135. Norris, D. I. R. *J. Nucl. Mater.* **1971**, *40*, 66–76.
136. Farrell, K.; Houston, J. T.; Wolfenden, A.; King, R. T.; Jostons, A. In *Radiation-Induced Voids in Metals, CONF-710601*; Corbett, J. W., Ianniello, L. C., Eds.; National Technical Information Service: Springfield, VA, 1972; pp 376–385.
137. Zinkle, S. J.; Farrell, K. *J. Nucl. Mater.* **1989**, *168*, 262–267.
138. Singh, B. N. *Nature* **1973**, *224*, 142–144.
139. Singh, B. N. *Philos. Mag.* **1974**, *29*, 25–42.
140. Singh, B. N.; Foreman, A. J. E. *Philos. Mag.* **1974**, *29*, 847–858.
141. Singh, B. N.; Leffers, T.; Green, W. V.; Green, S. L. *J. Nucl. Mater.* **1982**, *105*, 1–10.
142. Singh, B. N.; Leffers, T.; Green, W. V.; Victoria, M. *J. Nucl. Mater.* **1984**, *122–123*, 703–708.
143. Victoria, M.; Green, W. V.; Singh, B. N.; Leffers, T. *J. Nucl. Mater.* **1984**, *122–123*, 737–742.
144. Horsewell, A.; Singh, B. N. In *Twelfth International Symposium on Effect of Radiation on Materials*; Garner, F. A., Perrin, I. S., Eds.; American Society of Testing and Materials: Philadelphia, PA, 1985; ASTM STP 870, pp 248–261.
145. Foreman, A. J. E.; Singh, B. N.; Horsewell, A. *Mater. Sci. Forum* **1987**, *15–18*, 895–900.
146. Singh, B. N.; Horsewell, A. *J. Nucl. Mater.* **1994**, *212–215*, 410–415.
147. Horsewell, A.; Singh, B. N. *Influence of Grain and Subgrain Boundaries on Void Formation and Growth in Aluminum Irradiated with Fast Neutrons*; American Society of Testing and Materials: Philadelphia, PA, 1987; pp 220–229, ASTM Special Technical Publication 955.
148. Evans, J. H. *Nature* **1971**, *229*, 403–405.
149. Kulchinski, G. L.; Brimhall, J. L.; Kissinger, H. E. *J. Nucl. Mater.* **1971**, *40*, 166–174.
150. Wiffen, F. W. In *Proceedings of the International Conference on Radiation-Induced Voids in Metals*; Corbet, J. W., Iannielo, L. C., Eds.; U.S. Atomic Energy: Albany, NY, 1972; pp 386–396, USAEC-CONF-71061.
151. Mazey, D. J.; Francis, S.; Hudson, A. I. *J. Nucl. Mater.* **1973**, *47*, 137–142.
152. Risbet, A.; Levy, V. *J. Nucl. Mater.* **1974**, *50*, 116–118.
153. Loomis, B. A.; Gerber, S. B.; Taylor, A. *J. Nucl. Mater.* **1977**, *68*, 19–31.
154. Garner, A. F.; Stubbins, J. F. *J. Nucl. Mater.* **1994**, *212*, 1298–1302.
155. Horsewell, A.; Singh, B. N. *Radiat. Eff.* **1987**, *102*, 1–5.
156. Jäger, W.; Trinkaus, H. *J. Nucl. Mater.* **1993**, *205*, 394–410.
157. Foreman, A. J. E. *A Mechanism for the Formation of a Regular Void Array in an Irradiated Metal*; Harwell Report AERE-R 7135; 1972.
158. Hähner, P.; Frank, W. *Solid State Phenom. B* **1992**, *23–24*, 203–219.
159. Barashev, A. V.; Golubov, S. I. *Philos. Mag.* **2010**, *90*, 1787–1797.
160. Rowcliffe, A. F.; Lee, E. H. *J. Nucl. Mater.* **1982**, *108–109*, 306–318.
161. Pedraza, D. F.; Maziasz, P. J. Void-Precipitate Association During Neutron Irradiation of Austenitic Stainless Steel. In *Radiation-Induced Changes in Microstructure: 13th International Symposium (Part I), ASTM STP 955*; Garner, F. A., Packan, N. H., Kumar, A. S., Eds.; American Society for Testing and Materials: Philadelphia, 1987; pp 161–194.
162. Boothby, R. M.; Williams, T. M. *J. Nucl. Mater.* **1988**, *152*, 123–138.
163. Farrell, K.; Houston, J. T. *J. Nucl. Mater.* **1970**, *35*, 352–355.
164. Risbet, A.; Brebec, G.; Lanore, J. M.; Levy, V. *J. Nucl. Mater.* **1975**, *56*, 348–354.
165. Portnykh, I. A.; Kozlov, A. V.; Panchenko, V. L.; Chernov, V. M.; Garner, F. A. *J. Nucl. Mater.* **2007**, *367–370*, 925–929.
166. Golubov, S. I. *Metallofizika* **1989**, *11*, 10–18, [in Russian].
167. Golubov, S. I.; Ginkin, V. P.; Strokova, A. M. *Mater. Sci. Forum* **1992**, *97–99*, 97–103.